Review article

Advances in electrochemical sensors for naproxen detection: Mechanisms, performance factors, and emerging challenges

Seyed Saman Nemati [a], Gholamreza Dehghan [a,*], Jafar Soleymani [b],
Abolghasem Jouyban [b,c]

[a] Laboratory of Biochemistry and Molecular Biology, Department of Biology, Faculty of Natural Sciences, University of Tabriz, 51666-16471, Tabriz, Iran
[b] Pharmaceutical Analysis Research Center and Faculty of Pharmacy, Tabriz University of Medical Sciences, Tabriz, Iran
[c] Faculty of Pharmacy, Near East University, PO BOX: 99138 Nicosia, North Cyprus, Mersin, 10, Turkey

ARTICLE INFO

ABSTRACT

Naproxen (NAP), a nonsteroidal anti-inflammatory, analgesic, and antipyretic drug, has fewer side effects than similar drugs due to its aryl acetic acid structure. For this reason, it is widely prescribed to manage fever, short-term and long-term pain, and musculoskeletal disorders. However, its use has complications such as changes in kidney function, severe gastrointestinal lesions, and increased bleeding after surgery. In addition, the toxicity of NAP or its metabolites affects the organisms in the ecosystem. Therefore, it is necessary to determine the pharmaceutical quality of produced NAP and measure its amount in living organisms and the environment. Spectroscopy, chromatography, and electrochemical methods have been used to determine NAP. Electrochemical methods have attracted more attention due to their low cost, easy sample preparation, availability, sensitivity, and acceptable results. In addition, using nanomaterials for NAP oxidation results in high surface-to-volume, high available active sites, low cost, and long-term usability with high sensitivity. In this review, electrochemical-based methods for NAP analysis and sensing have been reviewed. Also, the influential factors in NAP identification and evaluation, and their oxidation mechanism have been discussed.

List of abbreviations

AMN	Methoxynaphtalene	GQD	Graphene quantum dots
BRB	Britton-Robinson buffer	MIP	Molecularly imprinted polymer
β-CD	β-Cyclodextrin	MWCNT	Multi-walled carbon nanotubes
CB-g	Carbon black grafted	NAP	Naproxen
CCE	Carbon ceramic electrode	LDH	Layered double hydroxide
CNF	Carbon nanofibers	LOQ	Limit of quantification
CNT	Carbon nanotubes	PAA	Polyacrylic acid
CNTPE	Carbon nanotube paste electrode	PANI	Polyaniline
CPE	Carbon paste electrode	PBS	Phosphate buffer saline
CB	Conduction band	rGO	Reduced graphene oxide
CV	Cyclic voltammetry	RSD	Relative standard deviation

(continued on next page)

* Corresponding author.
E-mail addresses: gdehghan@tabrizu.ac.ir, dehghan2001d@yahoo.com (G. Dehghan).

(continued)

DPV	Differential pulse voltammetry	SWV	Square wave voltammetry
DVD	Digital versatile disc	TBO	Toluidine blue O
FTO	Fluorine-doped thin oxide	VB	Valence band
GCE	Glassy carbon electrode		

1. Introduction

Naproxen (NAP) is a dicyclic propionic acid derivative that acts as a non-specific non-steroidal anti-inflammatory drug [1,2] (Fig. 1A). NAP is the inhibitor of cyclooxygenase isoforms in the synthesis pathway of prostacyclin, prostaglandins, and thromboxanes from arachidonic acid [1]. NAP is rapidly absorbed and has a long-lasting effect (13 h) due to its strong binding to plasma proteins. NAP is easily distributed in the synovial fluid and prescribed for arthritis patients. In addition, NAP consumption in a high dose compared to other nonsteroidal anti-inflammatory drugs and diclofenac results in a lower vascular risk [1,3]. In addition to the mentioned benefits, NAP can be obtained without a prescription, which is why it is widely used and more popular than similar drugs [4,5]. In contrast, recent research studies show long-term side effects of using NAP, including changes in kidney function, lesions, severe gastrointestinal ulcers, and increased bleeding after surgery [6–8]. In addition, NAP has been proposed as an emerging environmental pollutant [9,10]. NAP affects organisms in the ecosystem through the toxicity of NAP itself or its metabolites/degradation products. Toxic metabolites from NAP are formed through biological and physicochemical processes [11,12]. The photosynthetic derivatives of NAP have toxic effects on freshwater biome such as *Brachionus calyciflorus*, *Thamnocephalus platyurus*, *Ceriodaphnia dubia*, *Vibrio fischeri*, and *Daphnia magna* [11,13]. NAP photo derivatives with lower molecular weight, such as carbinol, ethyl, olefin, and ketone derivatives, have more toxic effects on bacteria than photo dimeric products [13]. Ma et al. [14], investigated the poisonous impact of NAP photodegradation products in *Vibrio fischeri* cells. The results showed that their toxicity was not increased due to the less spatial development and easy penetration of NAP derivatives. Of course, conflicting reports show a reduction in the toxicity of NAP derivatives resulting from light irradiation [11,15].

About 95 % of NAP from each dose is excreted in urine as NAP, 6-O-desmethyl naproxen, or their conjugates (more than 90 %) [16]. However, NAP can also be metabolized to NAP glucuronide [17] (Fig. 1B). Therefore, the concentration of NAP in urine and blood samples is determined through therapeutic drug monitoring as a clinical method of determining drug concentration in body fluids. On the other hand, the quality of the pharmaceutical product is a critical issue. Quality control should be done to ensure the safety and effectiveness of the drug; evaluate of drug's practical content during its preparation process, and measure the amount of the drug's active ingredient in the body [16]. Since NAP has been proposed as an environmental pollutant, efforts have been made to identify it in
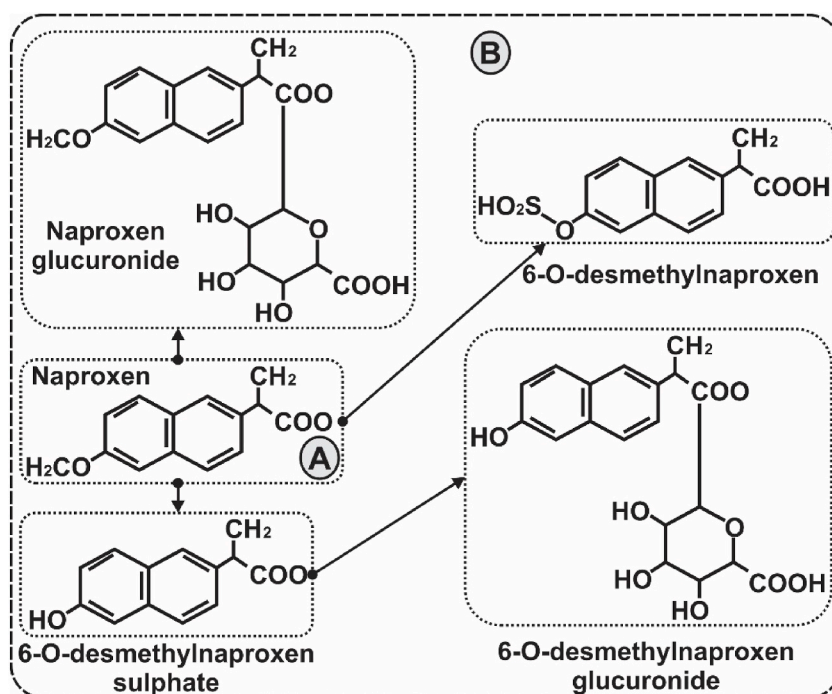

Fig. 1. (A) Chemical structure of NAP, (S)-6-methoxy-α-methyl-2-naphthalene acetic acid; (B) NAP is metabolized to O-desmethyl naproxen and its derivatives or NAP glucuronide.

the matrix [18,19]. Analytical methods such as electrochemical methods [20–22], high-performance liquid chromatography [23], thin-layer chromatography [24], synchronous spectroscopy [25], chemiluminescence [26,27], phosphorimetry [28], fluorimetry [29, 30], UV–vis spectrophotometry [31], and isotachophoresis [32] have been used to determine NAP concentration in the solution. Most reported methods for identifying NAP are time-consuming, require sample preconcentration, are expensive, and require derivatization. Therefore, developing cheap, sensitive, simple, and specific strategies to identify and determine the concentration of NAP is desirable [33].

Nanomaterials, with their unique physicochemical properties, have become the cornerstone of the advancements of industrial and diagnostic technologies and various scientific fields [34–40]. Incorporating nanostructured materials into diagnostic platforms has been welcomed due to their high surface-to-volume ratio, significantly enhanced reactivity, and tunable electrical and optical properties in sensors, especially optical and electrochemical [41]. The versatility of nanomaterials allows the design of sensors to detect a wide range of analytes [42,43]. Recent studies indicate nanocomposites in the structure of electrochemical and optical sensors for NAP detection [44].

Many recent studies have focused on optical [45–47] and electrochemical methods [48–50], and in the meantime, electrochemical methods have been more attractive to researchers as a fast-response, simple, and portable technique. Based on our best knowledge, there needs to be a review on identifying and estimating NAP concentration using electrochemical techniques. Therefore, NAP detection sensors will be examined from the point of view of detection ability, stability, reproducibility of results, effect of interfering substances, their applications in real samples, and mechanisms. We have collected documents related to NAP detection using electrochemical methods and then categorized them based on the nanomaterials used to modify electrodes. It tried to cover up all the available articles in this field and point out the possible strengths and weaknesses of the studies in construction methods, measurement parameters, environmental conditions, and proposed mechanisms. In this study, all the articles were reviewed with the same vision, and the final goal is to collect all the studies in this field until today.

2. Electrochemical sensors

Chemical sensors produce data through analyte concentration in the sample and complete sample analysis using proper analyzable signals [51,52]. The chemical sensor mainly consists of two parts: (1) a receptor and (2) a physicochemical converter [53,54]. The receptor interacts with the analyte, and the output signal will be formed due to chemical events (Fig. 2). Electrochemical methods are measurement techniques with a wide range of analytical possibilities. Electrochemistry, charge transfer between a specific electrode and a solid or liquid phase, includes the electrode interface reaction and the bulk solution's electrical conductivity [55,56]. Electrochemical sensors are the most widely used due to their high speed, inexpensive equipment, and meager detection limit [57]. Electrochemical sensors provide accurate real-time information from the analyte. Moreover, in ideal conditions, they have high reproducibility and reusability. The type of electrochemical sensor will be determined according to the nature of the analyte, the detection layer's sensitivity or selectivity, and the sample matrix's characteristics. Potentiometric (voltammetric) and amperometric electrochemical sensors are dominant [58,59]; however, amperometric sensors are used to detect electroactive chemical and biological analytes [60].

Electrochemical sensors include potentiometric, amperometric, photoelectrochemical, impedance, and electrochemiluminescence [53]. In the absence of convection, the transfer of charge carriers is due to the concentration gradient of electroactive species (diffusion current) or an electric field. In solutions, mass transport is due to an electric field. In potentiometric and amperometric techniques, net voltage and current in a closed loop are measured, respectively. Potentiometric methods usually use a two-electrode system, while in the amperometric method, a 3-electrode system is more common, and in some cases, a two-electrode system is used. At the same time, in impedimetric (conductivity), the conductivity of an electrochemical cell is determined [61]. Impedimetric sensors use surface impedance changes for analyte detection. In amperometric sensors, the sensor-analyte interaction causes the formation of a Nernst equilibrium at the sensor interface when there is no current in the system and provides information about the analyte concentration. By applying a specific voltage between the reference and work electrodes, amperometric sensors check the change in the resulting current due to electrochemical oxidation or reduction reactions according to the Cottrell equation [53]:
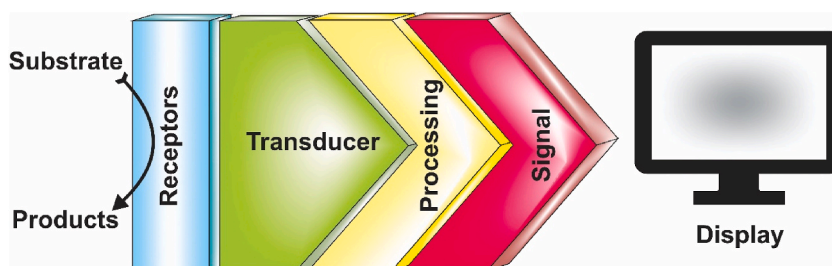

Fig. 2. Analyte (substrate) sensing path in electrochemical sensors. In the vicinity of the sensor receptors, the substrate is converted into a product, and the signals generated by chemical reactions are interpreted as the production or destruction of a specific ion/electrical charge, which is amplified by the transducer and, after analyzing it, into a signal.

$$i = \frac{nFAc_j^0 \sqrt{D_j}}{\sqrt{\pi t}}$$

Where i, n, F, A, c_j^0, D_j, and t are current (A), number of electrons, Faraday constant (96485 C/mol); area of the electrode in cm^2, initial concentration of the reducible analyte, the diffusion coefficient for species; and time (s), respectively.

Here, a brief overview of electrochemical sensors was presented. For a better understanding of the types of electrochemical sensors, refer to Ref. [62].

3. Role of nanomaterials in electrochemical sensors

The development of nanotechnology has positively impacted the sensor industry in recent decades [53,54]. Nanomaterials with attractive physicochemical properties and tiny dimensions have made it possible to study condensed matter physics [63–65]. Nanomaterials improve the sensitivity of sensors by increasing the desired molecular interaction potential [66,67]. For example, carbon-based nanomaterials are widely used in manufacturing chemical and biological sensors and have also been used in biomedical and pharmaceutical fields [68,69]. Nanocomposites increase sensor selectivity, sensitivity, and repeatability. Biocompatibility, high surface-to-volume ratio, adsorption capacity, and high reactivity have made nanocomposites attractive in the field of sensors [70]. Nanocomposites catalyze chemical reactions, help in molecular stabilization, and increase electron transfer and tagging of bio-molecules [71]. Graphene nanofibers [72], carbon nanotubes (CNTs) [73], conducting polymers [74], metal-organic frameworks
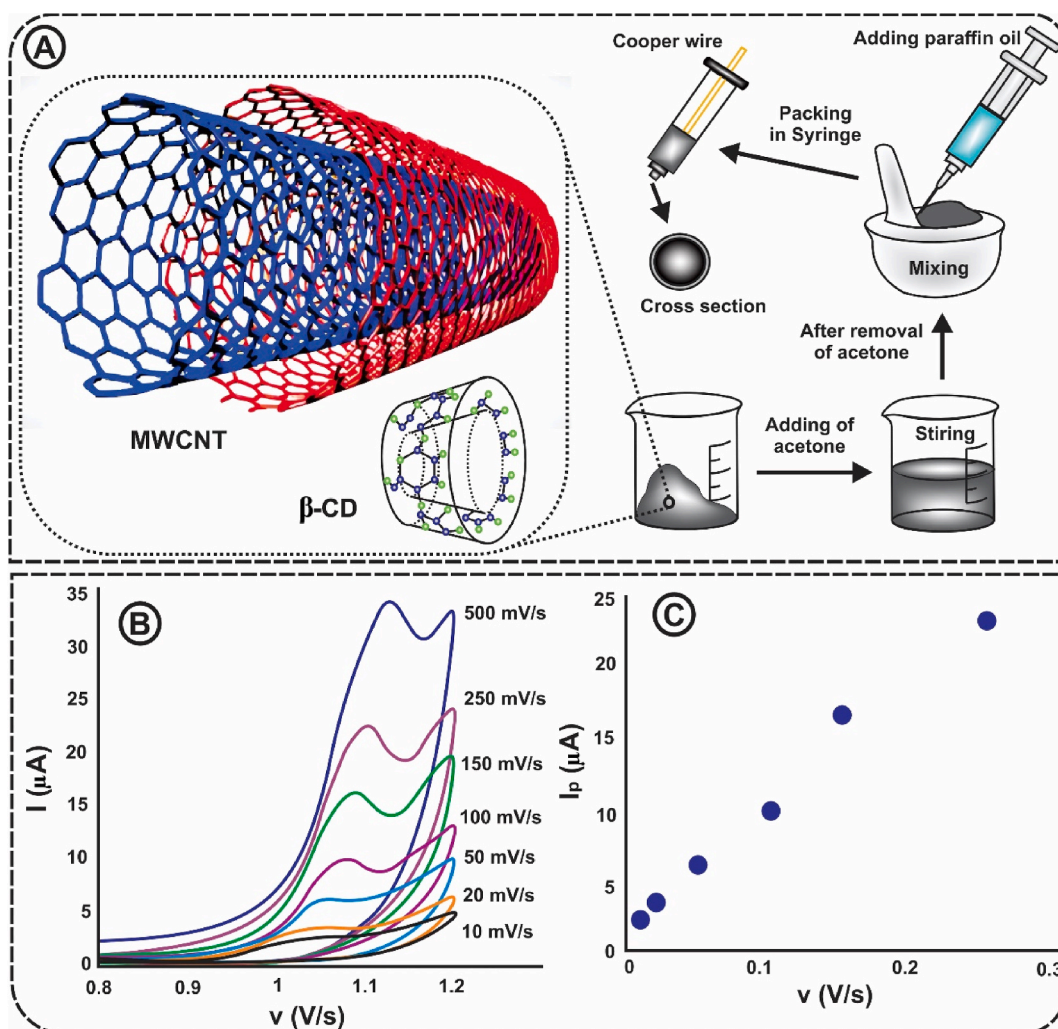

Fig. 3. (A) Schematic of the steps of preparation and synthesis of carbon nanotube paste electrode/β-cyclodextrin (CNTPE/β-CD) structure. (B) Cyclic voltammograms of CNTPE/β-CD under optimal conditions, ethanol: Britton-Robinson buffer (BRB) with a ratio of 1:10 (v/v), and pH 7, in the presence of 0.1 mM NAP; and (C) Peak current changes proportional to scan rate (further explanation in text) (Redrawn from Ref. [85]; with the permission of Copyright Clearance Center, order license ID: 1407928-1).

(MOFs) [75,76], nanoparticles [77], and nanocomposites [78] are the most common nanomaterials used in electrode modification. Using nanomaterials to modify electrodes improves the electrochemical responses of electrodes in detecting biological compounds and drugs [79]. Consequently, the studies have been divided based on the nature of nanomaterials used to modify the electrodes in the NAP electrochemical detection method and have been discussed.

3.1. Application of carbon-based materials

Carbon materials such as CNTs, fullerenes, graphene, activated carbon, and carbon nanofibers (CNFs) can improve the performance of electrochemical sensors due to their large surface area and good electrical conductivity [80]. CNTs have strong adsorption ability, excellent electrocatalytic activity, and high electrical conductivity [81,82]. In 2014, Montes et al. [83] used a glassy carbon electrode modified with multi-walled carbon nanotubes (MWCNT) for the electrochemical oxidation of NAP. MWCNT was responsible for the entrapment of NAP and the change in electrical parameters to detect NAP. Conversely, MWCNT had anti-fouling properties in NAP detection. This sensor's LOD and linear detection range for NAP were 6 μM and up to 200 μM, respectively. This study investigated the effects of scanning rate on NAP in MWCNT/GCE in phosphate buffer with pH 7.5. At rates of 10–100 mV s^{-1}, the peak NAP oxidation current was linear. The linearity of the oxidation current peak at low rates indicates that adsorption controls the oxidation process. On the other hand, the peak current of NAP oxidation at higher rates (up to 1000 mV s^{-1}) was also linear against the square root of the scan
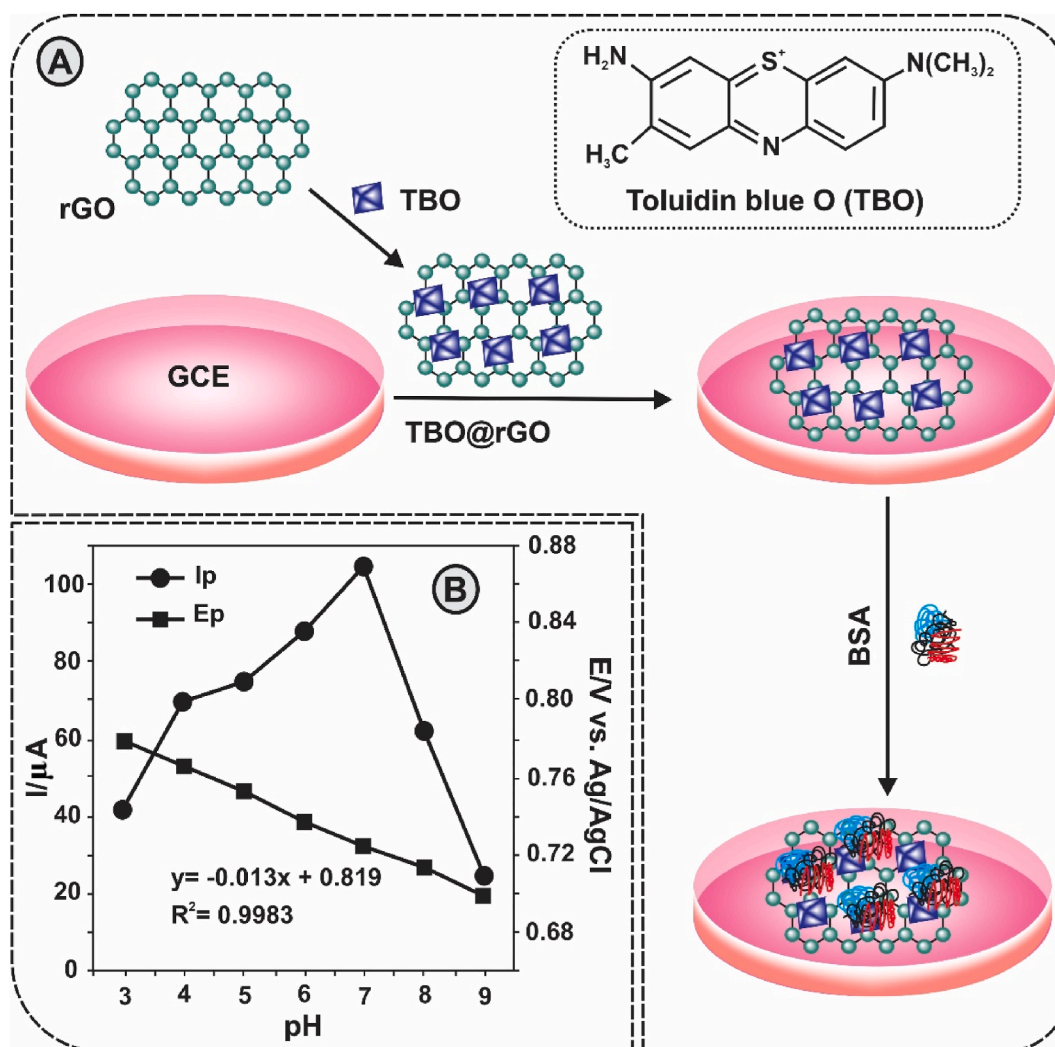

Fig. 4. (A) Schematic of modifying the glassy carbon electrode (GCE) surface by toluidine blue O (TBO), reduced graphene oxide (rGO), and bovine serum albumin (BSA). First, the rGO is modified by TBO, then the rGO/TBO layer is placed on the GCE surface. Next, the resulting surface is modified by BSA as a biomolecule (Redrawn from Ref. [87]; with the permission of Copyright Clearance Center, order license ID: 1407913-1). (B) Investigating the change in oxidation peak current and potential at pH 3–9 in 0.1 M Phosphate buffer saline (PBS) containing 0.5 mM NAP in poly (r-o-NBA)/GQDs/CPE electrode. The optimum pH for the electrode is 7 (more details in the text) (Redrawn from Ref. [91]; with the permission of Copyright Clearance Center, order license ID: 1407895-1).

rate. This study showed that the GCE electrode modified with MWCNT is more capable than the bare GCE electrode in detecting NAP. However, the ability of the sensor to detect NAP in real samples was not investigated. In another study, Baj-Rossi et al. [84] used drop-casting of MWCNT and microsomal cytochrome P4501A2 on a screen-printed electrode (SPE) to detect NAP. This sensor used cyclic voltammetry (CV) and amperometry to detect and determine the detection limit (16 μM) and the linear range of detection was 50–300 μM. This group had a promising innovation in using MWCNT and microsomal cytochrome P4501A2 on SPE for NAP detection; however, the obtained LOD was not ideal, and the stability of the sensor was low.

Afzali et al. [85] used CNT paste electrode/β-cyclodextrin (CNTPE/β-CD) for NAP electrochemical sensing. A schematic of the electrode preparation steps is shown in Fig. 3A. CNTPEs have several advantages over conventional CPEs, with good electrical conductivity, mechanical strength, electrocatalytic activity, high surface area, chemical stability, favorable electronic properties, and wide operation potential window. The linear range of this sensor for NAP was 0.4–23 μg/mL, and its LOD was 0.37 μg/mL. This study investigated the direct effect of scan rate on peak current and potential. The oxidation peak of aligned NAP shifted towards more positive values with the increase in peak current (Fig. 3B). The oxidation peak increased linearly with the scan rate in the 20–1000 mV s^{-1} (Fig. 3C), indicating that the kinetics of the redox reaction is an absorption-controlled process. Of course, the authors have shown voltammograms for the 10–500 mV s^{-1} range, but the current versus scan rate plot is 10–250 mV s^{-1}.

The excellent electronic, mechanical, biocompatibility and large surface area of graphene have led to biological applications and the use of graphene in electrochemical devices. Low bioactivity and low solubility are limiting factors of graphene, which can be overcome by using graphene modification with nanomaterials through covalent and non-covalent [86]. Guo et al. [87] developed a GCE electrode with toluidine blue O (TBO)-modified rGO as a basis for chiral selectivity by bovine serum albumin in detecting NAP.

TBO is a positively charged azine dye with high solubility and good electrical activity as a graphene probe with excellent redox properties. On the other hand, its positive charge facilitates the stabilization of negatively charged molecules on the surface of graphene (Fig. 4A). They used R-NAP and S-NAP enantiomers on separate sensors to investigate the enantioselectivity of the sensor. The results showed that the peak current of TBO oxidation decreased much more in the presence of R-NAP than S-NAP. These results show that R-NAP binds stronger than S-NAP to BSA on the surface of the biomarker electrode, and this is a major barrier to electron transfer in the vicinity of TBO. Therefore, the sensor is more likely to detect R-NAP. A LOD of 0.33 μM and a linear range of detection of 0.5–5 mM was reported for NAP. However, the innovation of this group in using the quenching effect of NAP on the BSA/TBO@rGO/GCE electrode surface is attractive [87].

In another study, Qian et al. [88] used graphene oxide (GO)-based composites for NAP sensing. In this study, boron doped reduced graphene oxide (B-rGO), nitrogen doped reduced graphene oxide (N-rGO), fluorine-doped reduced graphene oxide (F-GO), thermally reduced graphene oxide (Tr-rGO) and GO were used to modify GCE electrode. CV and DPV methods were used to measure NAP. The results showed that GCE@GO performed the best in NAP detection. The greater ability of the GCE@GO electrode in NAP detection than other electrodes was due to the higher oxygen content of GO, which facilitates the oxidation of NAP. The linear range of detection, LOD, the limit of quantification (LOQ), and the sensitivity of this sensor were 10–1000 μM, 1.94 μM, 6.74 μM and 0.6 μAμM^{-1}cm^{-2}, respectively. Also, the proposed sensor had a very good selectivity. The oxidation mechanism of NAP will be discussed in diagnosis mechanism section. This study has well reported the figures of merit (Linear range, LOD, LOQ, etc.) and has well stated the oxidation mechanism of NAP; however, optimization of scan speed in NAP assays and investigation of optimal pHs and capability factors, reusability, stability and reproducibility would make the report more complete.

Zero-dimensional composites, graphene quantum dots (GQDs), consist of single or multiple graphene layers with a thickness of less than 30 nm and a diameter of about 20 nm. GQDs modify electrodes such as CPE and GCE are very interesting because of the absence of electrode fouling on modified electrodes, low cytotoxicity, high surface area, and excellent solubility [89,90]. In this regard, Abd-Elsabour et al. [91] used CPE modified with GQDs loaded with reduced-o-nitrobenzoic acid (r-o-NBA) for NAP detection. Thin film of r-o-NBA polymer increases the modified electrode's reproducibility, stability, and active sites. In this study, LOD, LOQ, linear range of detection, and sensitivity were 0.67 μM, 2.24 μM, 1–100 μM and 0.42 μA μM^{-1} cm^{-2} respectively. Also, the effect of pH in the range of 3–9 on potential and peak current was investigated. As shown in Fig. 4B, the peak potential decreased with increasing pH, which shows that the proton is not depleted during the oxidation of NAP and the transfer of electrons occurs in the oxidation mechanism. On the other hand, the oxidation current peak reached at pH 7 was optimal. As expected, the presence of poly(r-o-NBA) increases the reproducibility and stability. The decrease in the sensor's efficiency in the presence of interfering substances was insignificant, and the recovery of the sensor was acceptable. Therefore, this comprehensive study investigated essential and validation factors of sensors' efficiency [91].

Carbon nanofibers (CNFs) are widely used in biological and electrochemical sensors due to their flexibility, excellent electrical conductivity, high surface area, and continuous structure [92–94]. Afzali et al. [92] developed a 1 butyl-3- methylimidazolium hexafluorophosphate (Bmim[PF$_6$]) CPE electrode modified with CNF/PANI (polyaniline) containing gold nanoparticles (Au NPs). Bmim [PF$_6$] is a green ionic liquid from organic anions and cations which make the electron transfer process faster. Combining PANI with carbon materials increases the number of capacitors and improves stability and conductivity of electrode surface. The Au NPs also increases electrocatalytic properties, electrical conductivity, and biocompatibility. This electrode had a detection range and LOD of 50–2000 μM and 16 μM, respectively. Increasing the scan rates from 8 to 400 mV s^{-1} did not change the oxidation peak potential, while it caused an increase in the oxidation peak current, proportional to the increase in the scan rate. In this study, the relationship between the square root of the scan rate and the oxidation peak current was linear in lower scan rates and a parabolic curve is obtained at high scan rates. Therefore, the mass transfer process influences the action mechanism of the electrode. Investigating the effect of pH in the range of 3–9 was similar to the findings of other articles, and the optimal pH was 7. The CNF/Au/PANI/CPE electrode in this proposed sensor had acceptable stability, reproducibility, and non-interference results. The reported LOD value for the developed system was high compared to similar studies, about 1 μM.

Carbon-based nanomaterials such as CNTs and graphene generally have an extensive surface area and excellent conductivity, which is suitable for sensitively detecting NAP at very low concentrations. On the other hand, due to the superb electron transfer properties, sensors based on non-carbon materials usually have a deficient response time. Another advantage of sensors based on carbon nanomaterials is compatibility with different platforms and high chemical and thermal stability. However, producing high-quality carbon nanomaterials is expensive, which limits the wide application of carbon nanomaterials in detecting NAP. On the other hand, using some carbon nanomaterials, especially certain types of CNTs, causes toxicity and limits their biomedical applications. On the other hand, it tends to accumulate, especially in aqueous environments, and the difficulty of functionalizing carbon-based nanomaterials is one of the other challenges of using carbon nanomaterials to detect NAP [95].

3.2. Metal-based materials

Transition metal oxides are widely used for electrochemical sensors due to their excellent electrocatalytic activity [96]. The low number of active sites of transition metal oxides such as CuO has limited their use in electrochemical sensors [97]. To solve this problem, doping and making composites containing metal oxides are usually used to synergize and improve the catalytic activity of metal oxides [97,98]. Prado and colleagues [99] coupled bismuth vanadate ($BiVO_4$) with CuO to design a photoelectrochemical sensor to detect NAP. The semiconductor $BiVO_4$ increases the efficiency of the photocurrent generated during the oxidation of NAP. $BiVO_4$/CuO nanocomposite showed high-efficiency for modification of fluorine-doped thin oxide (FTO) glass electrode. Under visible light irradiation, first, an electron is released in the oxidation process of NAP, and the semiconductor valence band holes capture the released electron. In the following, the deprotonated form of NAP forms an uncharged, decarboxylated radical and loses an electron to form a cation that is stabilized by the resonance structures of the methoxy naphthyl ring. Conversely, the second electron produced in this process is cleared by the holes of the semiconductor's valence band. The filling of the valence band (VB) holes by these electrons causes the electrons promoted to the conduction band (CB) to be transferred to the converter, and the optical current will increase in proportion to the NAP concentration (Fig. 5). The detection limit and linear detection range of the $BiVO_4$/CuO/FTO electrode for NAP were 5 and 5–480 nM, respectively. The optimal pH for NAP assay by $BiVO_4$/CuO/FTO was 6.3. The LOD values and linear range reported by this study are in the nanomolar scale. On the other hand, the lack of influence of interfering substances on the measurement results, repeatability after ten times measurement, and high recovery power, indicate the high efficiency of the $BiVO_4$/CuO/FTO photoelectrochemical sensor to detect NAP.

In another study, Taherizadeh et al. [97] modified CPE electrode with the peony-like CuO: Tb^{3+} nanostructure (P-LCuO: Tb^{3+}) and

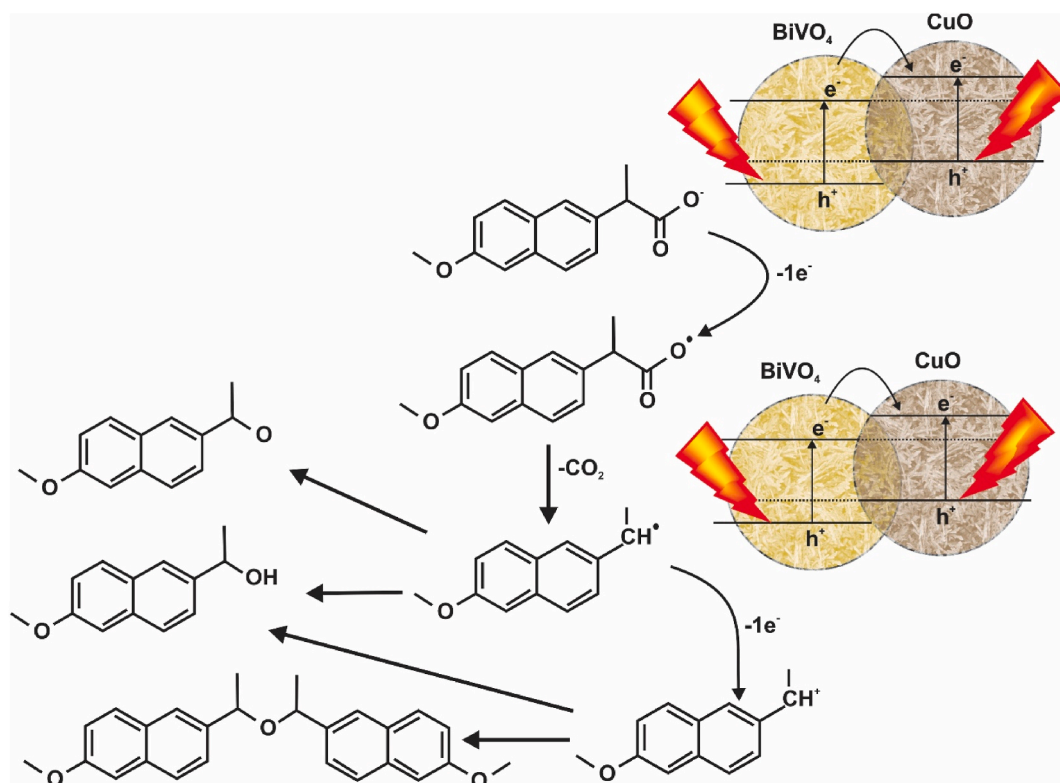**Fig. 5.** Schematic of the steps of photoelectrochemical detection of NAP by $BIVO_4$/CuO/FTO electrode. The general mechanism is similar to the primary mechanism of NAP oxidation in electrochemical sensors, except that the measurement is based on the change of light intensity (more details in the text) (Redrawn from Ref. [99]; with the permission of Copyright Clearance Center, license number: 5651900516834).

used the modified electrode for the electrochemical detection of NAP and sumatriptan. CuO is a semiconductor with impressive electrochemical properties used as a substitute for precious metals and their oxides. The main limitation of CuO in electrochemical sensors is lack of active sites in its structure. Due to its high catalytic activity, high chemical stability, and easy oxidation, Tb in states Tb^{III} and Tb^{IV}, was used to doping CuO for enhancing ionic conductivity. CV, DPV, and chronoamperometry techniques were used for electrochemical analysis. The LOD and linear detection range of the P-LCuO: Tb^{3+} electrode for NAP was 2.7 nM and 0.01–700 μM, respectively. The optimum pH was 6 for the NAP assay, and the effect of scanning speed on the peak oxidation current indicates the control of oxidation by diffusion. The sensor based on the P-LCuO:Tb^{3+} electrode had good reproducibility and recovery. On the other hand, the assay in the presence of ionic and organic interferences showed no interference in the results of the NAP assay. In another study, Kanagasabapathy et al. [100] used nano spinel ferrite films ($ZnFe_2O_4$) for the electrochemical detection of NAP by chronoamperometric and chronopotentiometric techniques. The LOD and LOQ of this sensor were 0.13 μM and 0.41 μM, respectively, which are weak results compared to other electrodes modified with metals.

Afkhami et al. [101] used the Au NP placed on the modified gold electrode with L-cysteine self-assembled monolayers to analyze the enantiomeric compounds of the chiral NAP compound. Schematic of Electrode preparation is shown in Fig. 6A. Cyclic voltammograms of Au/Au NPs-Cys under optimal conditions for 2.5 mM [Fe (CN)$_6$]$^{4-/3-}$ (scan rate 100 mV s^{-1}) are shown in Fig. 6B. A more significant decrease in the redox peaks was observed when for S-NAP, indicating an excellent absorption for S-NAP compared to the R-NAP to the electrode surface, creating a more substantial barrier to prevent electron transfer. The optimal pH for the oxidation potential and peak current was 6 (Fig. 6C). Also, the optimal time range for the NAP reaction with AuNPs-modified electrode was 5–30 min. Increasing the interaction time in both enantiomers results in a more considerable current change. However, at times longer than 20 min, there was no noticeable change in the current (Fig. 6D). Therefore, the optimal interaction time was 20 min The results showed that increasing the concentration of both R-NAP and S-NAP enantiomers in the 2–20 μM range will change the anodic peak linearly. Although increasing the concentration of both enantiomers caused a change in the oxidation peak current, the slope of the line in the detection linear range was higher for S-NAP than for R-NAP. Therefore, it can be seen that the sensor acts selectively for the S-NAP enantiomer. Compared with previous studies [87] in which the enantioselectivity of NAP assessed by TBO@rGO/GCE electrochemical sensor, the linear range and LOD were different from Au/AuNPs/Cys sensor. However, the selectivity coefficient of the Au/AuNPs/Cys sensor for S-NAP is twice that of the TBO@rGO/GCE sensor.

Mutharani et al. studied carbon black (CB)-decorated lanthanum oxide (La_2O_3) nanomaterials grafted on polyacrylic acid (PAA) nano gel (CB-g-PAA/La_2O_3) for simultaneous determination of NAP, theophylline, and acetaminophen. The detection linear range and
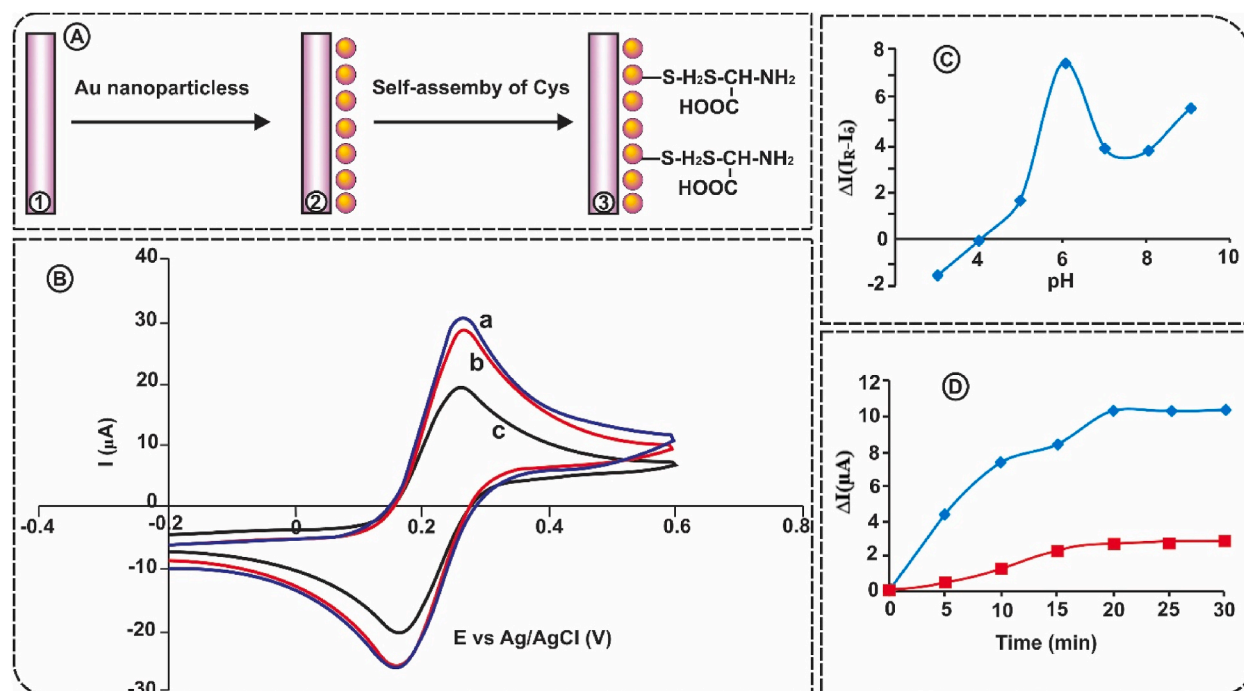

Fig. 6. (A) Schematic of the fabrication process of Au/AuNPs/Cys chiral electrode surface, (1) bare Au electrode, (2) Au electrode modified with gold nanoparticles, (3) Au/AuNPs electrode after immobilization of L-cysteine self-assembly on it; (B) CV for Au/AuNPs/Cys electrode in the presence of 2.5 mM [Fe(CN)$_6$]$^{4-/3-}$ (a), incubated with 100 mg/L R-NAP (b) and S-NAP (c) (test conditions: 20 min incubation, pH 6, scan rate 100 mV s^{-1}, scan potential −0.20 to 0.6 V vs. Ag/AgCl) (Redrawn from Ref. [101]; with the permission of Copyright Clearance Center, order license ID: 1407883-1); **(C)** The dependence of peak current changes on pH in Au/AuNPs/Cys electrode; and (D) Optimal time for detection of S-NAP (blue) and R-NAP (red) enantiomers by Au/AuNPs/Cys sensor(Redrawn from Ref. [101]; with the permission of Copyright Clearance Center, order license ID: 1407890-1).

LOD of CB-g-PAA/La$_2$O$_3$/GCE electrode for NAP detection were 0.05–884 μM and 35 nM, respectively. Moreover, the measurement of NAP in blood serum and urine samples indicated the high recovery power of CB-g-PAA/La$_2$O$_3$/GCE [102].

Recently, Ghanavati et al. [103] used ZnO, NiO, and Fe$_3$O$_4$ to decorate MWCNTs on GCE electrodes to detect NAP and sumatriptan simultaneously. Nanocomposite in this study was used to improve the diversity of oxidation peaks to detect drugs simultaneously. ZnO/NiO/Fe$_3$O$_4$/MWCNTs/GCE had high efficiency for NAP detection. Therefore, the LOD and linear detection range were 3 nM and 0.004–350 μM, respectively. NAP with a concentration of 12 μM in 0.1 M phosphate buffer solution (pH 7) was investigated in the scan speed range of 10–400 mV s^{-1} to investigate the effect of scan speed on electrode performance. Data showed that increasing the scanning speed causes a shift in the potential and current peaks to higher values. Also, the linear relationship between peak current and voltage showed that the mass transfer of drugs on the electrode was controlled by diffusion. The reproducibility, reusability, and recovery (in human serum and urine samples) of ZnO/NiO/Fe$_3$O$_4$/MWCNTs/GCE were acceptable. The results of this study show that modifying the electrode with a combination of carbon and metal oxide nanomaterials improves various detection parameters compared to using carbon materials individually on the surface of the electrode. For example, in this study, the LOD was in the nM range, while in the carbon-based sensors, in the detection of NAP, the LOD was in the μM range [83,84,87].

According to the examined examples, sensors based on metal nanoparticles improve the sensitivity and detection limit of electrochemical sensors. Their high catalytic activity improves the possibility of analyte detection. They also have good versatility and can tolerate a wider pH range. However, aggregation issues reduce the performance of metal-based nanomaterials. In addition, it is not easy to control the conditions during their synthesis, and nanoparticles with different sizes may be produced, which reduces reproducibility [77].

3.3. Other materials

Cyclodextrins are other popular materials in electrochemical sensors [104]. The incomplete conical structure of cyclodextrin has given them unique chemical and physical properties [105]. It incorporates cyclodextrins with guest molecules to form inclusion complexes. Cyclodextrins and drugs interact through the hydrophilic outer surface and lipophilic inner cavity, weak electrostatic interactions, hydrogen bonding, dipole-dipole, van der Waals forces, and steric effects [106]. Tarahomi et al. [107] modified a gold digital versatile disc (G-DVD) with Ag NPs@Graphene oxide-β-cyclodextrin. The innovation of this group was to use cheap DVDs as gold source electrodes. AgNPs@GO-β-CD/G-DVD electrode's LOD, LOQ, and detection linear range for NAP detection were 23 nM, 80 nM, and 0.4–80 μM, respectively. The techniques used in this study were CV and differential pulse voltammetry (DPV). Drugs with similar structures, organic materials, and common ions in the body did not interfere with NAP detection process; moreover, the recovery of the electrode was defensible. In another study, Lenik and Łyszczek [20] used neutral cyclodextrins such as heptakis (tri-O-methyl)-β-cyclodextrin and cyclodextrin anionic chloride 2-hydroxy-3-N, N, N-trimethylamino)propyl-β-cyclodextrin to develop NAP potentiometric sensor. Cyclodextrin polymer made selectivity towards the target molecule. The results revealed that the developed system has excellent selectivity for NAP in comparison with other ions. The β-CD electrode had a LOD and linear detection range of 10 μM and 50 mM to 10 mM, which is not acceptable compared to other methods discussed in this review.

Molecularly imprinted polymers (MIPs) have high chemical stability and selectivity, which makes them attractive in sensors with high selectivity [108]. The electrodes modified with MIP in the nanoscale improve the electrochemical activity due to increased surface area, the number of reactive sites on the surface, and the three-dimensional structure [109]. Rajabi et al. [49] used MIP to modify the CPE electrode surface for the potentiometric detection of NAP. NAP as a template, methacrylic as a functional monomer, and ethylene glycol dimethacrylate as a crosslinker were used to construct MIP. The resulting sensor detected NAP with a LOD and detection linear range of 0.3 nM and $1 \times 10^{-9.5}$– 1×10^{-1} M, respectively. In order to investigate the effect of pH on NAP measurement, concentrations of 1, 0.1, and 0.01 NAP were used in the pH 3–13. Based on the results in the pH 5–11, the electrode's response was linear, while at pH less than 5, a significant change in potential occurred due to the decrease in the concentration of NAP as a weak acid. Also, at a pH higher than 11, due to the hydroxide groups, interference is caused in the operation of the sensor. Conversely, the MIP/CPE optimal response time for measuring NAP in different concentrations was about 3 s, while other studies in this field required a higher response time. For example, the response times for NAP in the studies of Norouzi et al. [110], Pezza et al. [111], and Lenik et al. [112] were 20 s, 10–35 s, and 15–20 s, respectively. The fast response time of MIP/CPE is due to the nano MIP structure with a large surface area and high propensity to print. Also, the stability, reusability, and recovery of the sensor was acceptable [49]. In another study, Eslami and Alizadeh [21] used pyrrole monomer to construct MIP for NAP detection. First, the MIP was fabricated, fixed on a quartz microbalance gold electrode, and used for the electrochemical measurement of NAP. This electrode had a LOD of 30 nM. The results of this study showed that the selectivity of the modified electrode for NAP is proportional to the controlled oxidation of conductive MIP. On the other hand, the oxidation rate of conductive MIP depends on the pH value of the solution. Over-oxidation occurs at low potentials in alkaline media, but alkaline media are unsuitable due to damage to the microbalance-modified quartz gold electrode. However, controlled oxidation starts with a more positive potential in an acidic medium. Therefore, a pH higher than 7.4 is not recommended for this electrode.

MIP-based electrochemical sensors improved sensitivity and had high selectivity. Due to their versatility, stability, and durability, they are recommended for naproxen diagnostic sensors. However, hard optimization, such as polymerization conditions and monomer selection, pattern removal challenges that sometimes cause false positives, and the difficulty of production at the level of abundance are the challenges of MIP-based electrochemical sensors [113].

3.4. Chiral nanomaterials

Enantioselective detection of naproxen enantiomers (NAP) using chiral nanomaterials is a promising approach in electrochemical sensing that takes advantage of the unique properties of these materials to increase the sensitivity and selectivity of use. Chiral nanomaterials can create specific binding sites and prefer one enantiomer. For example, Afkhami et al. [101], exploited the difference in the interaction of NAP enantiomers with a chiral-modified electrode surface. This study investigated a gold electrode modified with gold nanoparticles and L-cysteine monolayers to investigate the interaction between S-NAP and R-NAP using CV and EIS techniques. The results showed better interaction of S-NAP than R-NAP with the sensor. The difference in the generated signal was attributed to the different interactions of NAP enantiomers with the modified chiral electrode surface [101]. In another study, Jafari et al. [114], investigated the electrochemical response of S-NAP and R-NAP on a glass electrode modified with graphene oxide and L-cysteine. In this study, EIS and CV techniques were used for diagnosis. The results showed that the proposed sensor selectively detects S-NAP in the presence of R-NAP. One of the noteworthy points of this study is that by increasing the electrode interaction time with enantiomers from 5 min to 30 min, the difference between peak currents for the selective measurement of S-NAP increased compared to R-NAP. The linear detection range for both enantiomers was 5.0×10^{-6}-1.3×10^{-4} M, and the detection limit for S-NAP and R-NAP was 3.5×10^{-7} and 2.5×10^{-6} M, respectively. Graphene-based nanocomposites facilitate the rapid absorption of NAP enantiomers while increasing reproducibility and stability [114]. The development of NAP electrochemical sensors based on chiral nanomaterials enables the precise enantioselective analysis of NAP compounds and helps to improve the physician's precise drug monitoring.

4. Mechanism of detection

The main mechanism for detecting NAP in electrochemical process was single step oxidation [83,115,116]. Other studies confirm the mechanism presented based on the pre-institutional path in Fig. 7. In the study of Rodrigo et al., MWCNT immobilized on GCE was developed for NAP detection. This study used square wave voltammetry (SWV) to determine NAP in MWCNT/GCE. After SWV calculations, two steps of single-electron transfer were obtained. The results of this study were contrary to all previous studies on the NAP oxidation mechanism because, in previous studies, an electron transfer step was considered during the oxidation process, which included electron transfer and decarboxylation. Subsequent studies have all confirmed the results of this two-step electron transfer mechanism for NAP oxidation [83].

Qian et al. [88], used bare graphene oxide (GO) and fluorine-doped GO, partially boron-reduced GO, thermally reduced GO and
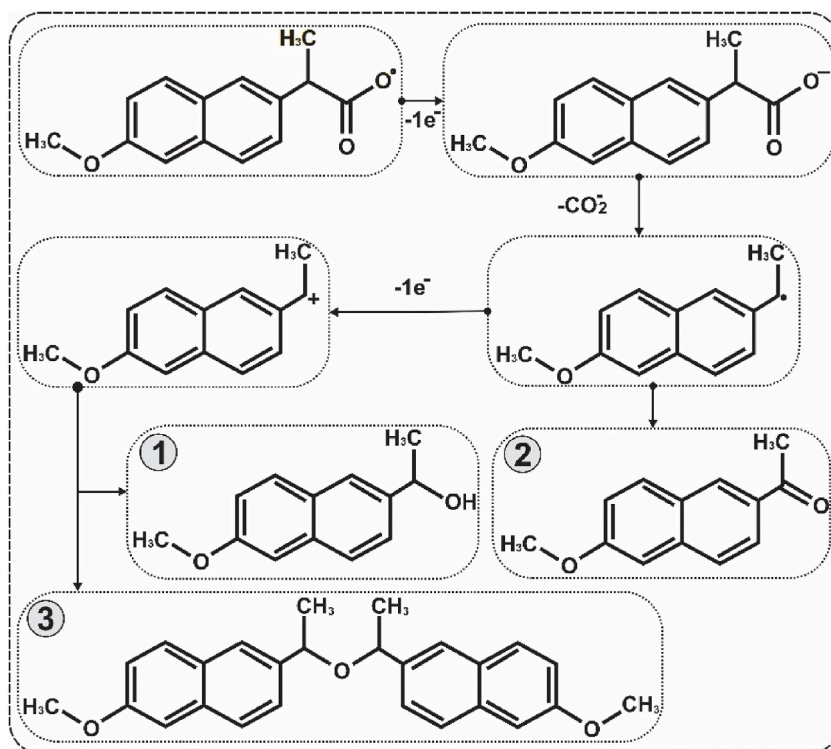
Fig. 7. Schematic of the NAP oxidation process: At a neutral medium, NAP is completely deprotonated, and a free radical is formed during the oxidation and then decarboxylation process. Then, in the second step of one-electron transfer, the cation formed by methoxy will be stabilized by methoxy-naphthyl ring resonance, which is supported by the isolated products (1, 2, and 3). (Redrawn from Ref. [83]; with the permission of Copyright Clearance Center, license number: 5651911488192).

partially nitrogen-reduced GO for electrochemical detection of NAPs. Their study showed that bare GO is more effective for NAP detection than other GO-based nanomaterials used in this study. GO is more efficient in the catalytic oxidation of NAP due to the presence of additional oxygens. The CV curve indicates NAP oxidation with peaks around 0.86 and 1.17 V. During anionic oxidation, a radical of NAP formed in the first peak, and in the second peak, ketone (2-acetyl-6-methoxynaphthalene) was formed due to further oxidation. They also used the DPV technique for more clarity. Indeed, in DPV, the background current is limited, and the resolution is higher due to the much higher decay rate of the capacitive current than the faradaic current. The first main product occurs following its decarboxylation. Initially, NAP catalytically oxidized to NAP oxide on the electrode surface. Then, by intermediate decarboxylation, the final product of the NAP oxidation pathway, i.e., ketone (2-acetyl-6-methoxynaphthalene), will be produced. In this project, the authors have ignored one of the peaks, and the chemical structure presented for the oxidation mechanism of naproxen is maybe incorrect [88]. As shown in Fig. 8A, CV curves have two peaks. The first peak (0.86 V) was attributed to the electrochemical oxidation of naproxen, while the peak (1.17 V) was attributed to further oxidation of cationic radicals to form ketones. Also, Fig. 8B shows the DPV that attributed the first peak to NAP decarboxylation and ignored the second peak.

Hung et al. modified the GCE electrode with rGO and via the anodic electropolymerization of poly-(L-serine) (PLS) and used for NAP detection in the water. Hydroxide radicals produced during PLS/rGO-Nafion/GCE fabrication accelerate NAP decarboxylation. At the same time, the surface of PLS/rGO-Nafion will be regenerated to form intermediate cationic NAP radicals in the aromatic ring. Oxidation, decarboxylation, deprotonation, and an uncharged radical of 2-methyl 6-ethoxy naphthalene will be produced at the first step of electrooxidation. Then, the methoxy naphthyl ring will create a stabilized cation through resonance structures and nucleophilic attack to transfer the second electron. Finally, 2-acetyl-6-methoxynaphthalene (AMN) will be produced as the main product, and 2-methoxy-6-ethylnaphthalene (MEN) and 1-(6-methoxy-2-naphthyl)ethanol (MNE) in lesser amount (Fig. 9) [117]. The mechanism leading to the production of MNE and MEN compounds has also been reported by other groups [85,118]. Also, other groups have reported a similar mechanism to identify naproxen in the mechanism leading to AMN [99,119].

In another study, Suryanarayanan et al. used boron-doped diamond electrodes for NAP detection using CV and DPV techniques. In order to investigate the reaction mechanism, NAPs were used in a solution containing CH_3CN and $LiClO_4$ on a boron-doped diamond electrode. The UV–visible spectrum was used to monitor the electrolysis process. NAP had two distinct λ_{max} values at 273 and 331.5 nm, which did not change during the electrolysis process and even at the end of the reaction. However, the height of the anodic voltammetry peak decreased during coulometry and turned into a background current at the end of electrolysis. The amount of electricity consumed was proportional to the electron process and the first step of electrooxidation. Next, comprehensive NAP electrolysis was performed, and the contents of the loaded solution on the electrode were dried and analyzed by 1H NMR spectrum. The results showed the presence of the acetamide group (NHCOMethyl) in the α-carbon of the NAP side chain. Also, a small amount of product was observed when substituting acetamide in the aromatic ring of NAP. Therefore, the general mechanism proposed was as follows: the electrochemical reaction of one-electron oxidation of NAP and cationic radicals is formed in the aromatic cores [118].

5. Comparison of electrochemical and other NAP sensors

In addition to sensors based on electrochemistry, diagnostic methods such as colorimetry and fluorescence are used to detect NAP [45,46,120]. Fluorescent nanomaterials such as gold nanoclusters (AuNCs) have opened the door for nanomaterials in fluorescence sensors [121]. AuNCs have attracted attention due to their small size, wavelengths comparable to Fermi conduction electrons, and molecular properties in experiments based on aging spectra. It is worth mentioning that AuNCs will emit high fluorescence by a single layer of inactive organic molecules [122]. In this regard, Jafari et al. [123] used AuNCs stabilized with bovine serum albumin (BSA) to detect the S- and R- NAP. The fluorescence quenching in the presence of the S-NAP was more than that of the R-NAP. The linear detection range of S- and R- NAP was 0.74–9.1 μM and 9.1–31 μM, respectively. In addition, the LOD of the sensor for S- and R- NAP
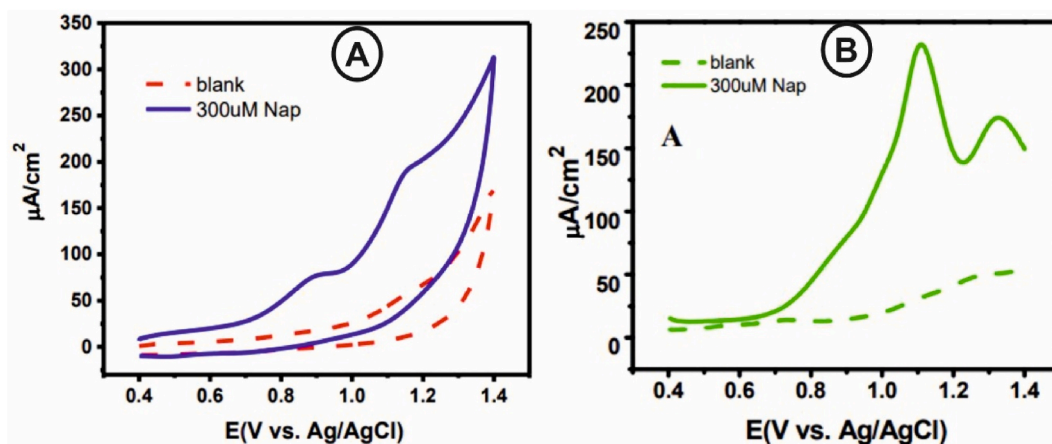

Fig. 8. CV (A) and DPV (B) of GO-based electrochemical sensor of NAP in the absence and presence of NAP (300 μ M). Condition: PBS buffer 0.1 M, pH 7.2 [88].
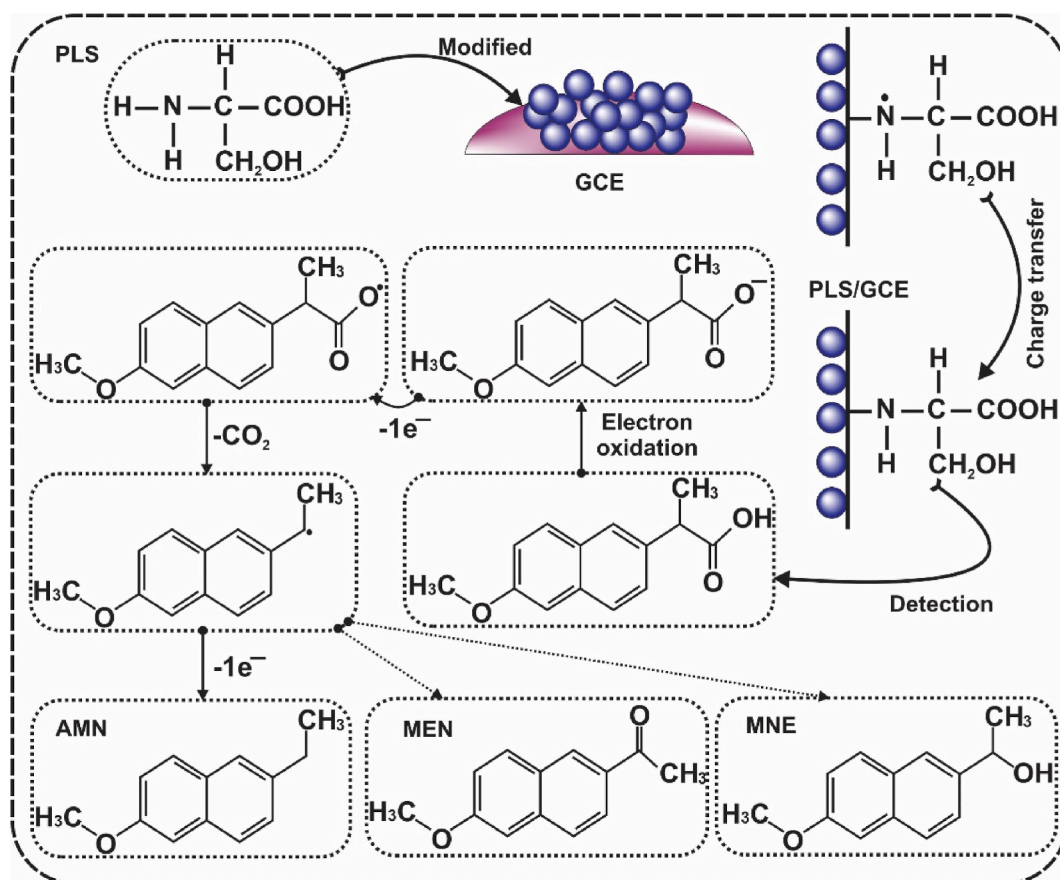
Fig. 9. Electrochemical reaction mechanism of NAP on PLS/rGO-Nafion/GCE. The mechanism is performed as two single electron transfers and decarboxylation (2-methoxy-6-ethylnaphthalene (MEN); 2-acetyl-6-methoxynaphtalene (AMN)), (more details in the text) (Redrawn from Ref. [117]; with the permission of Copyright Clearance Center, license number: 5651900971539).

was 0.74 μM and 0.95 μM. According to the report of this group, the designed sensor had high stability (data not available), and the pH had no direct effect on the performance of the sensor.

Deep eutectic solvents are safe and inexpensive green solvents with 2–3 components linked together by hydrogen bonding. The

Table 1
A comparison between electrochemical and non-electrochemical NAP sensors in LOD, linear range of detection, and recovery power in the measurement of real samples.

Material	Method of Detection	LOD (nM)	Linear range (μM)	Real Sample Recovery (%)	Ref.
Electrochemistry					
FeNi$_3$/CuS/BiOCl/CPE	CV, DPV	60	0.2–500	96.2–104.9 (urine)	[50]
Al$_2$O$_3$/GCE	BIA, amperometry	12	0.05–0.5	–	[127]
P-L CuO: Tb^{3+} NS/CPE	CV, DPV	2.7	−700	98.2–99.4 (serum) 99.4–100.9 (urine)	[97]
CB-g-PAA/La$_2$O$_3$	CV, DPV	35	0.05–884	98.5–99.5 (serum) 97-100 (urine)	[102]
DyNW/CPE	Voltammetry	0.5	1–5	97-101 (urine)	[128]
Non-electrochemistry					
N, S, Cl/CDs + Fe$^{(III)}$	Spectroscopy	25	0.05–70	97-104 (serum)	[47]
CDs-SiO$_2$@MIP	Spectroscopy	200	0.5–35	101–101.4 (serum)	[46]
Tβ-CD-Au NPs	Colorimetry	2.6	0.017–0.781	99-104 (serum)	[16]
C$_{18}$ silica gel	Fluorometry	1.3	0.004–0.108	96.1–104 (serum)	[129]
molecularly imprinted CD	Fluorometry	30	0.05–4	95-101 (Simulative urine)	[45]

Batch-injection analysis (BIA); Carbon black (CB); **C**arbon dots (CD); Conducting molecularly imprinted polypyrrole (CMIP); Carbon paste electrode (CPE); Cyclic voltammetry (CV); Dysprosium nanowire modified (DyNW); Differential pulse voltammetry (DPV); Electrochemical impedance spectroscopy (EIS); Molecularly imprinted polymer (MIP); Peony-Like CuO: Tb^{3+} nanostructures (P-L CuO: Tb^{3+} NS); Poly (acrylic acid) (PAA); quartz crystal microbalance (QCM); and Thiolated β-cyclodextrin (Tβ-CD).

melting point of eutectic solvents is lower than its components, and they have the advantage of high biocompatibility, low toxicity, and low radiation [124]. Eutectic solvents improve the surface characteristics, make doping of heteroatoms possible, and improve the optical properties of carbon quantum dots [125,126]. Tabaraki et al. [47] used a deep eutectic solvent to synthesize sulfur, nitrogen, and chloride-doped carbon dots. The fluorescence quenching method in the interaction between carbon quantum dots with Fe(III) was used to measure NAP. The sensor's linear detection range and LOD for NAP assay were 0.05 μM–70 μM and 25 nM, respectively. This sensor had the same efficiency in the pH range of 4–6, and its efficiency decreased above pH 6. It is noticeable, that the activity level of the sensor in the real serum sample had a recovery efficiency of 97–104 %. Table 1 shows some critical parameters in the validation of electrochemical NAP sensors and other types in different studies. As it turns out, in all cases, the NAP electrochemical sensors perform equally or even better than the other types.

6. Challenges and future Perspectives

Here, the potential of electrochemical sensors in NAP detection and recent developments are reviewed. However, there are still challenges that will be fascinating to face in the future. Despite the promising results, the high selectivity of NAP electrochemical sensors is still a challenge. Of course, care must be taken that the methods used to increase selectivity do not decrease sensitivity. Using MIP to increase selectivity, without reducing sensitivity, is an ideal option. For example, in similar electrochemical sensors, Wang et al. [130], used SiO_2@MIP combined with MWCNTs for dibutyl phthalate sensing and developed a sensor with high selectivity and sensitivity.

In some cases, nanocomposites used in electrochemical sensors do not justify the correct reason for the choice. The selected nanocomposites should have synergistic or multifunctional properties that will ultimately lead to the development of compounds with high oxidation power, high electron transfer capability, good conductivity, and high surface-to-volume ratio. The use of new and up-to-date nanomaterials in this field can be very useful; for example, the use of dichalcogenides, MXenes and carbon nitride in the sensitive layer of the electrochemical sensor is attractive [131]. The correct selection of nanocomposite components can also effectively improve the stability of sensors in harsh conditions. For example, Li et al. [132], used poly(pyrrole) polymerization on black phosphorus nanosheets modified with Au NPs to detect pefloxacin. The stability of the developed nanocomposite was much higher than bare black phosphorus. Therefore, more attention should be paid to the correct selection of nanocomposite components in developing a stable NAP electrochemical sensor in the future. Of course, electrochemical sensors based on FETs will also be effective for the greater stability of NAP electrochemical sensors. In FETs, by stabilizing the sensing layer using synthesis techniques such as CVD and sol-gel on the surface of the sensing layers, the nanocomposites will be stable for repeated uses, as well as the entire FET device, design They usually have very good stability and reproducibility [43].

Another challenge of electrochemical sensing platforms is their integration with the Internet of Things (IoT), artificial intelligence, and machine learning. Although emerging technologies have been integrated into other electrochemical sensors [133], this still needs to be done for NAP electrochemical sensors.

7. Conclusion

In conclusion, electrochemical sensors offer a fascinating solution for naproxen analysis, characterized by fast response time, reasonable price, and high sensitivity. Incorporating nanocomposites, especially those based on metal oxides and carbon materials, significantly increases the performance of these sensors and makes them very effective for naproxen sensing. However, despite these advances, several challenges still need to be solved in optimizing the stability, selectivity, and integration of emerging technologies with existing electrochemical systems. Continued development of more reliable and efficient naproxen electrochemical sensors, especially in healthcare applications where accurate monitoring of drug levels for patient safety and treatment efficacy requires further attention. In addition, ongoing research on the mechanisms of naproxen oxidation and factors affecting its detection will help refine these technologies. They are overcoming the current limitations and increasing the capabilities of sensors, diagnostic accuracy, and environmental monitoring, ultimately leading to better health outcomes and environmental protection.

CRediT authorship contribution statement

Seyed Saman Nemati: Writing – original draft, Methodology, Investigation, Data curation. **Gholamreza Dehghan:** Writing – review & editing, Supervision, Project administra. **Jafar Soleymani:** Writing – review & editing, Investigation. **Abolghasem Jouyban:** Writing – review & editing.

Data availability statement

No data was used for the research described in the article.

Declaration of competing interest

The authors declare that they have no known competing financial interests or personal relationships that could have appeared to influence the work reported in this paper.

Appendix A. Supplementary data

Supplementary data to this article can be found online at https://doi.org/10.1016/j.heliyon.2024.e40906.

References

[1] C.A. Barcella, M. Lamberts, P. McGettigan, E.L. Fosbøl, J. Lindhardsen, C. Torp-Pedersen, G.H. Gislason, A.M.S. Olsen, Differences in cardiovascular safety with non-steroidal anti-inflammatory drug therapy—a nationwide study in patients with osteoarthritis, Basic Clin. Pharmacol. Toxicol. 124 (5) (2019) 629–641.

[2] D. Wojcieszyńska, U. Guzik, Naproxen in the environment: its occurrence, toxicity to nontarget organisms and biodegradation, Appl. Microbiol. Biotechnol. 104 (2020) 1849–1857.

[3] D.J. Angiolillo, S.M. Weisman, Clinical pharmacology and cardiovascular safety of naproxen, Am. J. Cardiovasc. Drugs 17 (2017) 97–107.

[4] A. Dzionek, D. Wojcieszyńska, K. Hupert-Kocurek, M. Adamczyk-Habrajska, U. Guzik, Immobilization of Planococcus sp. S5 strain on the loofah sponge and its application in naproxen removal, Catalysts 8 (5) (2018) 176.

[5] C.M. Aguilar, I. Chairez, J.L. Rodríguez, H. Tiznado, R. Santillán, D. Arrieta, T. Poznyak, Inhibition effect of ethanol in naproxen degradation by catalytic ozonation with NiO, RSC advances 9 (26) (2019) 14822–14833.

[6] T. Madrakian, M. Ahmadi, A. Afkhami, M. Soleimani, Selective solid-phase extraction of naproxen drug from human urine samples using molecularly imprinted polymer-coated magnetic multi-walled carbon nanotubes prior to its spectrofluorometric determination, Analyst 138 (16) (2013) 4542–4549.

[7] A. Aresta, F. Palmisano, C.G. Zambonin, Determination of naproxen in human urine by solid-phase microextraction coupled to liquid chromatography, J. Pharmaceut. Biomed. Anal. 39 (3–4) (2005) 643–647.

[8] T. Martinez-Sena, S. Armenta, M. de la Guardia, F.A. Esteve-Turrillas, Determination of non-steroidal anti-inflammatory drugs in water and urine using selective molecular imprinted polymer extraction and liquid chromatography, J. Pharmaceut. Biomed. Anal. 131 (2016) 48–53.

[9] T. Kosjek, E. Heath, A. Krbavčič, Determination of non-steroidal anti-inflammatory drug (NSAIDs) residues in water samples, Environ. Int. 31 (5) (2005) 679–685.

[10] L. Araujo, J. Wild, N. Villa, N. Camargo, D. Cubillan, A. Prieto, Determination of anti-inflammatory drugs in water samples, by in situ derivatization, solid phase microextraction and gas chromatography–mass spectrometry, Talanta 75 (1) (2008) 111–115.

[11] N. Jallouli, K. Elghniji, O. Hentati, A.R. Ribeiro, A.M. Silva, M. Ksibi, UV and solar photo-degradation of naproxen: TiO2 catalyst effect, reaction kinetics, products identification and toxicity assessment, J. Hazard Mater. 304 (2016) 329–336.

[12] C.E. Rodríguez-Rodríguez, A. Jelić, M. Llorca, M. Farré, G. Caminal, M. Petrović, D. Barceló, T. Vicent, Solid-phase treatment with the fungus Trametes versicolor substantially reduces pharmaceutical concentrations and toxicity from sewage sludge, Bioresour. Technol. 102 (10) (2011) 5602–5608.

[13] M. DellaGreca, M. Brigante, M. Isidori, A. Nardelli, L. Previtera, M. Rubino, F. Temussi, Phototransformation and ecotoxicity of the drug Naproxen-Na, Environ. Chem. Lett. 1 (2003) 237–241.

[14] D. Ma, G. Liu, W. Lv, K. Yao, X. Zhang, H. Xiao, Photodegradation of naproxen in water under simulated solar radiation: mechanism, kinetics, and toxicity variation, Environ. Sci. Pollut. Control Ser. 21 (2014) 7797–7804.

[15] R. Marotta, D. Spasiano, I. Di Somma, R. Andreozzi, Photodegradation of naproxen and its photoproducts in aqueous solution at 254 nm: a kinetic investigation, Water Res. 47 (1) (2013) 373–383.

[16] J. Khodaveisi, A.M.H. Shabani, S. Dadfarnia, D. Saberi, A novel sensor for determination of naproxen based on change in localized surface plasmon peak of functionalized gold nanoparticles, Spectrochim. Acta Mol. Biomol. Spectrosc. 179 (2017) 11–16.

[17] R. Addison, S. Parker-Scott, W. Hooper, M. Eadie, R. Dickinson, Effect of naproxen co-administration on valproate disposition, Biopharm Drug Dispos. 21 (6) (2000) 235–242.

[18] A.L.M. Ríos, K. Gutierrez-Suarez, Z. Carmona, C.G. Ramos, L.F.S. Oliveira, Pharmaceuticals as emerging pollutants: case naproxen an overview, Chemosphere 291 (2022) 132822.

[19] J.-M. Brozinski, M. Lahti, A. Meierjohann, A. Oikari, L. Kronberg, The anti-inflammatory drugs diclofenac, naproxen and ibuprofen are found in the bile of wild fish caught downstream of a wastewater treatment plant, Environmental Science & Technology 47 (1) (2013) 342–348.

[20] J. Lenik, R. Łyszczek, Functionalized β-cyclodextrin based potentiometric sensor for naproxen determination, Mater. Sci. Eng. C 61 (2016) 149–157.

[21] M.R. Eslami, N. Alizadeh, Nanostructured conducting molecularly imprinted polypyrrole based quartz crystal microbalance sensor for naproxen determination and its electrochemical impedance study, RSC Adv. 6 (12) (2016) 9387–9395.

[22] L. Zagitova, Y. Yarkaeva, V. Zagitov, M. Nazyrov, S. Gainanova, V. Maistrenko, Voltammetric chiral recognition of naproxen enantiomers by N-tosylproline functionalized chitosan and reduced graphene oxide based sensor, J. Electroanal. Chem. 922 (2022) 116744.

[23] N. Sahoo, M. Sahu, P. Rao, G. Ghosh, Development and validation of liquid chromatography-mass spectroscopy/mass spectroscopy method for quantitative analysis of naproxen in human plasma after liquid-liquid extraction, Trop. J. Pharmaceut. Res. 13 (9) (2014) 1503–1510.

[24] A. Pyka, E. Wiatr, K. Kwiska, D. Gurak, Validation thin layer chromatography for the determination of naproxen in tablets and comparison with a pharmacopeil method, J. Liq. Chromatogr. Relat. Technol. 34 (10–11) (2011) 829–847.

[25] H.M. Maher, Simultaneous determination of naproxen and diflunisal using synchronous luminescence spectrometry, Journal of Fluorescence 18 (2008) 909–917.

[26] M. Kamruzzaman, A.-M. Alam, K.M. Kim, S.H. Lee, Y.H. Kim, S.H. Kim, Silver nanoparticle-enhanced chemiluminescence method for determining naproxen based on Europium (III)-sensitized Ce (IV)-Na 2 S 2 O 4 reaction, Journal of fluorescence 22 (2012) 883–890.

[27] C.-Y. Wang, B. Yu, H. Fu, P. Wang, C.-C. Wang, A mixed valence Tb (III)/Tb (IV) metal-organic framework: crystal structure, luminescence property and selective detection of naproxen, Polyhedron 159 (2019) 298–307.

[28] G. Zhu, H. Ju, Determination of naproxen with solid substrate room temperature phosphorimetry based on an orthogonal array design, Anal. Chim. Acta 506 (2) (2004) 177–181.

[29] E.-P. Zisiou, P.C. Pinto, M.L.M. Saraiva, C. Siquet, J.L. Lima, Sensitive sequential injection determination of naproxen based on interaction with β-cyclodextrin, Talanta 68 (2) (2005) 226–230.

[30] M.A. Meetani, A. Alhalabi, M.K. Al-Tabaji, A. Al-Hemyari, H.A. Saadeh, N.i. Saleh, Cucurbituril—assisted sensitive fluorescence detection and quantitation of naproxen drug in wastewater samples: guest-host characterization and HPLC investigation, Front. Chem. 10 (2022) 1093231.

[31] N. Alizadeh, F. Keyhanian, Simple, sensitive and selective spectrophotometric assay of naproxen in pure, pharmaceutical preparation and human serum samples, Acta Poloniae Pharmaceutica-Drug Research 72 (5) (2015) 867–875.

[32] J. Sádecká, M. Čakrt, A. Hercegová, J. Polonský, I. Skačáni, Determination of ibuprofen and naproxen in tablets, J. Pharmaceut. Biomed. Anal. 25 (5–6) (2001) 881–891.

[33] K. Sarhangzadeh, Application of multi wall carbon nanotube–graphene hybrid for voltammetric determination of naproxen, J. Iran. Chem. Soc. 12 (2015) 2133–2140.

[34] N. Rashidi, M.J.S. Fard, P. Hayati, J. Janczak, F. Yazdian, S. Rouhani, T.A. Msagati, Antibacterial and cytotoxicity assay of two new Zn (ii) complexes: synthesis, characterization, X-ray structure, topology, Hirshfeld surface and thermal analysis, J. Mol. Struct. 1231 (2021) 129947.

[35] M. Aghaee, K. Mohammadi, P. Hayati, P. Sharafi-Badr, F. Yazdian, A.G. Alonso, S. Rostamnia, F. Eshghi, A novel 3D Ag (I) metal-organic coordination polymer (Ag-MOCP): crystallography, Hirshfeld surface analysis, antibacterial effect and molecular docking studies, J. Solid State Chem. 310 (2022) 123013.

[36] M.J.S. Fard, P. Hayati, H.S. Naraghi, S.A. Tabeie, Synthesis and characterization of a new nano lead (II) 0-D coordination supramolecular compound: a precursor to produce pure phase nano-sized lead (II) oxide, Ultrason. Sonochem. 39 (2017) 129–136.

[37] Z. Akbari, M. Montazerozohori, S.J. Hoseini, R. Naghiha, P. Hayati, G. Bruno, A. Santoro, J.M. White, Synthesis, crystal structure, Hirshfeld surface analyses, antimicrobial activity, and thermal behavior of some novel nanostructure hexa-coordinated Cd (II) complexes: precursors for CdO nanostructure, Appl. Organomet. Chem. 35 (5) (2021) e6181.

[38] P. Hayati, A. Gutiérrez, The role of non-covalent interactions on supramolecular assembly of coordination compounds of mercury (II) based on substituted pyridine mixed ligands. A survey of different conditions on morphology of new flower and ribbon like submicro structures, Inorg. Chim. Acta. 479 (2018) 83–96.

[39] M.K. Mohammadi, A. Gutierrez, P. Hayati, K. Mohammadi, R. Rezaei, Diverse structural assemblies and influence in morphology of different parameters in a series of 0D and 1D mercury (II) metal–organic coordination complexes by sonochemical process, Polyhedron 160 (2019) 20–34.

[40] S.S. Nemati, G. Dehghan, A. Khataee, L. Alidokht, N. Kudaibergenov, Layered double hydroxides as versatile materials for detoxification of hexavalent chromium: mechanism, kinetics, and environmental factors, J. Environ. Chem. Eng. (2024) 114742.

[41] S.S. Nemati, G. Dehghan, Photoelectrochemical biosensors: prospects of graphite carbon nitride-based sensors in prostate-specific antigen diagnosis, Anal. Biochem. (2024) 115686.

[42] S.S. Nemati, M.H.S. Seresht, G. Dehghan, Y. Abdi, An innovative sensor for sensitive determination of phenobarbital in real samples using CeO 2/CuO/MnO and CeO 2/CuO/NiO ion-sensitive field effect transistors, IEEE Sensor. J. (2024) 29651–29658.

[43] S.S. Nemati, G. Dehghana, N. Sheibani, Y. Abdi, Ion-sensitive field effect transistors-based biosensors: the sources of gates and their sensitive layers-A Review, IEEE Sensor. J. (2024) 17324–17336.

[44] S.S. Nemati, M. Salemi-Seresht, Y. Abdi, G. Dehghan, Highly sensitive and label-free detection of naproxen using mixed metal oxide-based field effect transistor as a biosensor for in-vitro analysis of urine, Mater. Sci. Semicond. Process. 179 (2024) 108487.

[45] K. Li, M. Zhang, X. Ye, Y. Zhang, G. Li, R. Fu, X. Chen, Highly sensitive and selective detection of naproxen via molecularly imprinted carbon dots as a fluorescent sensor, RSC advances 11 (46) (2021) 29073–29079.

[46] Z. Dehghani, M. Akhond, G. Absalan, Carbon quantum dots embedded silica molecular imprinted polymer as a novel and sensitive fluorescent nanoprobe for reproducible enantioselective quantification of naproxen enantiomers, Microchem. J. 160 (2021) 105723.

[47] R. Tabaraki, F. Nazari, Fluorescent nanoprobe for detection of naproxen based on doped carbon dots prepared in choline chloride-thiourea deep eutectic solvent, J. Iran. Chem. Soc. (2023) 1–8.

[48] C.-M. Hung, C. Huang, S.-K. Chen, C.-W. Chen, C.-D. Dong, Electrochemical analysis of naproxen in water using poly (L-serine)-modified glassy carbon electrode, Chemosphere 254 (2020) 126686.

[49] H.R. Rajabi, A. Zarezadeh, Development of a new chemically modified carbon paste electrode based on nano-sized molecular imprinted polymer for selective and sensitive determination of naproxen, J. Mater. Sci. Mater. Electron. 27 (2016) 10911–10920.

[50] P. Mohammadzadeh Jahani, H. Akbari Javar, H. Mahmoudi-Moghaddam, Development of a novel electrochemical sensor using the FeNi 3/CuS/BiOCl nanocomposite for determination of naproxen, J. Mater. Sci. Mater. Electron. 31 (2020) 14022–14034.

[51] A. Hulanicki, S. Glab, F. Ingman, Chemical sensors: definitions and classification, Pure Appl. Chem. 63 (9) (1991) 1247–1250.

[52] H. Imanzadeh, A. Khataee, L. Hazraty, M. Amiri, Broken hollow carbon spheres decorated by gold nanodendrites as the advanced electrochemical sensing platform for sensitive tracing of morphine in human serum and saliva, Sensor. Actuator. B Chem. 398 (2024) 134738.

[53] J. Baranwal, B. Barse, G. Gatto, G. Broncova, A. Kumar, Electrochemical sensors and their applications: a review, Chemosensors 10 (9) (2022) 363.

[54] S.S. Nemati, G. Dehghan, S. Rashtbari, T.N. Tan, A. Khataee, Enzyme-based and enzyme-free metal-based glucose biosensors: classification and recent advances, Microchem. J. (2023) 109038.

[55] B.-M. Țuchiu, R.-I. Stefan-van Staden, J.F. van Staden, Recent trends in ibuprofen and ketoprofen electrochemical quantification–a review, Crit. Rev. Anal. Chem. 54 (1) (2024) 61–72.

[56] H. Sohrabi, F. Maleki, P. Khaaki, M. Kadhom, N. Kudaibergenov, A. Khataee, Electrochemical-based sensing platforms for detection of glucose and H2O2 by porous metal-organic frameworks: a review of status and prospects, Biosensors 13 (3) (2023) 347.

[57] N.P. Shetti, D.S. Nayak, K.R. Reddy, T.M. Aminabhvi, Graphene–clay-based hybrid nanostructures for electrochemical sensors and biosensors, in: Graphene-based Electrochemical Sensors for Biomolecules, Elsevier, 2019, pp. 235–274.

[58] E.G. Neiva, M.F. Bergamini, M.M. Oliveira, L.H. Marcolino Jr., A.J. Zarbin, PVP-capped nickel nanoparticles: synthesis, characterization and utilization as a glycerol electrosensor, Sensor. Actuator. B Chem. 196 (2014) 574–581.

[59] M.D. Meti, J.C. Abbar, J. Lin, Q. Han, Y. Zheng, Y. Wang, J. Huang, X. Xu, Z. Hu, H. Xu, Nanostructured Au-graphene modified electrode for electrosensing of chlorzoxazone and its biomedical applications, Mater. Chem. Phys. 266 (2021) 124538.

[60] L. Tong, L. Wu, E. Su, Y. Li, N. Gu, Recent advances in the application of nanozymes in amperometric sensors: a review, Chemosensors 11 (4) (2023) 233.

[61] T. Dodevska, D. Hadzhiev, I. Shterev, Electrochemical sensors for the safety and quality control of cosmetics: an overview of achievements and challenges, J. Electrochem. Sci. Eng. 14 (1) (2024) 3–35.

[62] E. Bakker, M. Telting-Diaz, Electrochemical sensors, Analytical chemistry 74 (12) (2002) 2781–2800.

[63] A. Şenocak, V. Sanko, S.O. Tümay, Y. Orooji, E. Demirbas, Y. Yoon, A. Khataee, Ultrasensitive electrochemical sensor for detection of rutin antioxidant by layered Ti3Al0. 5Cu0. 5C2 MAX phase, Food Chem. Toxicol. 164 (2022) 113016.

[64] N. Pourshirband, A. Nezamzadeh-Ejhieh, Experimental design on determination of Sn (II) by the modified carbon paste electrode with Fe (II)-exchanged clinoptilolite nanoparticles, Solid State Sci. 99 (2020) 106082.

[65] N. Pourshirband, A. Nezamzadeh-Ejhieh, The boosted activity of AgI/BiOI nanocatalyst: a RSM study towards Eriochrome Black T photodegradation, Environ. Sci. Pollut. Control Ser. 29 (30) (2022) 45276–45291.

[66] M. Negahdary, L. Angnes, Application of electrochemical biosensors for the detection of microRNAs (miRNAs) related to cancer, Coord. Chem. Rev. 464 (2022) 214565.

[67] B. Pérez-Fernández, A. de la Escosura-Muniz, Electrochemical biosensors based on nanomaterials for aflatoxins detection: a review (2015–2021), Anal. Chim. Acta 1212 (2022) 339658.

[68] B. Pérez-López, A. Merkoçi, Nanomaterials based biosensors for food analysis applications, Trends Food Sci. Technol. 22 (11) (2011) 625–639.

[69] F. Sanchez, K. Sobolev, Nanotechnology in concrete–a review, Construct. Build. Mater. 24 (11) (2010) 2060–2071.

[70] S. Shrivastava, N. Jadon, R. Jain, Next-generation polymer nanocomposite-based electrochemical sensors and biosensors: a review, TrAC, Trends Anal. Chem. 82 (2016) 55–67.

[71] R. Batool, A. Rhouati, M.H. Nawaz, A. Hayat, J.L. Marty, A review of the construction of nano-hybrids for electrochemical biosensing of glucose, Biosensors 9 (1) (2019) 46.

[72] M.A. Kanjwal, A.A. Ghaferi, Graphene incorporated electrospun nanofiber for electrochemical sensing and biomedical applications: a critical review, Sensors 22 (22) (2022) 8661.

[73] A. Palumbo, Z. Li, E.-H. Yang, Trends on carbon nanotube-based flexible and wearable sensors via electrochemical and mechanical stimuli: a review, IEEE Sensor. J. (2022) 20102–20125.

[74] A. Dinu, C. Apetrei, A review of sensors and biosensors modified with conducting polymers and molecularly imprinted polymers used in electrochemical detection of amino acids: phenylalanine, tyrosine, and tryptophan, Int. J. Mol. Sci. 23 (3) (2022) 1218.

[75] H.-W. Zhang, H.-K. Li, Z.-Y. Han, R. Yuan, H. He, Incorporating fullerenes in nanoscale metal–organic matrixes: an ultrasensitive platform for impedimetric aptasensing of tobramycin, ACS Appl. Mater. Interfaces 14 (5) (2022) 7350–7357.

[76] M. Daniel, G. Mathew, M. Anpo, B. Neppolian, MOF based electrochemical sensors for the detection of physiologically relevant biomolecules: an overview, Coord. Chem. Rev. 468 (2022) 214627.

[77] K. Białas, D. Moschou, F. Marken, P. Estrela, Electrochemical sensors based on metal nanoparticles with biocatalytic activity, Microchim. Acta 189 (4) (2022) 172.

[78] H. Kaur, S.S. Siwal, R.V. Saini, N. Singh, V.K. Thakur, Significance of an electrochemical sensor and nanocomposites: toward the electrocatalytic detection of neurotransmitters and their importance within the physiological system, ACS Nanoscience Au 3 (1) (2022) 1–27.

[79] B. Nigović, S. Jurić, A. Mornar, Electrochemical determination of nepafenac topically applied nonsteroidal anti-inflammatory drug using graphene nanoplatelets-carbon nanofibers modified glassy carbon electrode, J. Electroanal. Chem. 817 (2018) 30–35.

[80] P. Gopal, T.M. Reddy, Fabrication of carbon-based nanomaterial composite electrochemical sensor for the monitoring of terbutaline in pharmaceutical formulations, Colloids Surf. A Physicochem. Eng. Asp. 538 (2018) 600–609.

[81] S. Islam, S. Shaheen Shah, S. Naher, M. Ali Ehsan, M.A. Aziz, A.S. Ahammad, Graphene and carbon nanotube-based electrochemical sensing platforms for dopamine, Chem.–Asian J. 16 (22) (2021) 3516–3543.

[82] H. Karimi-Maleh, H. Beitollahi, P.S. Kumar, S. Tajik, P.M. Jahani, F. Karimi, C. Karaman, Y. Vasseghian, M. Baghayeri, J. Rouhi, Recent advances in carbon nanomaterials-based electrochemical sensors for food azo dyes detection, Food Chem. Toxicol. 164 (2022) 112961.

[83] R.H. Montes, J.S. Stefano, E.M. Richter, R.A. Munoz, Exploring multiwalled carbon nanotubes for naproxen detection, Electroanalysis 26 (7) (2014) 1449–1453.

[84] C. Baj-Rossi, T.R. Jost, A. Cavallini, F. Grassi, G. De Micheli, S. Carrara, Continuous monitoring of Naproxen by a cytochrome P450-based electrochemical sensor, Biosens. Bioelectron. 53 (2014) 283–287.

[85] F. Afzali, G. Rounaghi, M.H.A. Zavar, N. Ashraf, Supramolecular β-cyclodextrin/multi-walled carbon nanotube paste electrode for amperometric detection of naproxen, J. Electrochem. Soc. 163 (3) (2015) B56.

[86] S. Kumar, S.D. Bukkitgar, S. Singh, Pratibha, V. Singh, K.R. Reddy, N.P. Shetti, C. Venkata Reddy, V. Sadhu, S. Naveen, Electrochemical sensors and biosensors based on graphene functionalized with metal oxide nanostructures for healthcare applications, ChemistrySelect 4 (18) (2019) 5322–5337.

[87] L. Guo, Y. Huang, Q. Zhang, C. Chen, D. Guo, Y. Chen, Y. Fu, Electrochemical sensing for naproxen enantiomers using biofunctionalized reduced graphene oxide nanosheets, J. Electrochem. Soc. 161 (4) (2014) B70.

[88] L. Qian, A.R. Thiruppathi, R. Elmahdy, J. van der Zalm, A. Chen, Graphene-oxide-based electrochemical sensors for the sensitive detection of pharmaceutical drug naproxen, Sensors 20 (5) (2020) 1252.

[89] T. Ghiasi, S. Ahmadi, E. Ahmadi, M.R.T.B. Olyai, Z. Khodadadi, Novel electrochemical sensor based on modified glassy carbon electrode with graphene quantum dots, chitosan and nickel molybdate nanocomposites for diazinon and optimal design by the Taguchi method, Microchem. J. 160 (2021) 105628.

[90] H. Rageh, M. Abdel-sabour, Pharmaceutical electrochemistry: the electrochemical behaviour of paracetamol at ZnO nanoparticales/1, 2-napthaquinone-4-sulphonic acid glassy carbon modified electrode, Anal Bioanal Electrochem 9 (3) (2017) 351–364.

[91] M. Abd-Elsabour, M.M. Abou-Krisha, A.G. Alhamzani, T.A. Yousef, An effective, novel, and cheap carbon paste electrode for naproxen estimation, Rev. Anal. Chem. 41 (1) (2022) 168–179.

[92] M. Afzali, Z. Jahromi, R. Nekooie, Sensitive voltammetric method for the determination of naproxen at the surface of carbon nanofiber/gold/polyaniline nanocomposite modified carbon ionic liquid electrode, Microchem. J. 145 (2019) 373–379.

[93] T. Yan, Z. Wang, Y.-Q. Wang, Z.-J. Pan, Carbon/graphene composite nanofiber yarns for highly sensitive strain sensors, Mater. Des. 143 (2018) 214–223.

[94] E. Arkan, G. Paimard, K. Moradi, A novel electrochemical sensor based on electrospun TiO2 nanoparticles/carbon nanofibers for determination of Idarubicin in biological samples, J. Electroanal. Chem. 801 (2017) 480–487.

[95] D. Maiti, X. Tong, X. Mou, K. Yang, Carbon-based nanomaterials for biomedical applications: a recent study, Front. Pharmacol. 9 (2019) 1401.

[96] X. Zhang, Q. Xiao, Y. Zhang, X. Jiang, Z. Yang, Y. Xue, Y.-M. Yan, K. Sun, La2O3 doped carbonaceous microspheres: a novel bifunctional electrocatalyst for oxygen reduction and evolution reactions with ultrahigh mass activity, J. Phys. Chem. C 118 (35) (2014) 20229–20237.

[97] M. Taherizadeh, S. Jahani, M. Moradalizadeh, M.M. Foroughi, Carbon paste modified with peony-like CuO: Tb3+ nanostructures for the simultaneous determination of sumatriptan and naproxen in biological and pharmaceutical samples, ChemistrySelect 8 (1) (2023) e202203152.

[98] J.D. Rodney, S. Deepapriya, M.C. Robinson, C.J. Raj, S. Perumal, B.C. Kim, S.J. Das, Lanthanum doped copper oxide nanoparticles enabled proficient bi-functional electrocatalyst for overall water splitting, Int. J. Hydrogen Energy 45 (46) (2020) 24684–24696.

[99] T.M. do Prado, C.C. Badaró, R.G. Machado, P.S. Fadini, O. Fatibello-Filho, F.C. Moraes, Using bismuth vanadate/copper oxide nanocomposite as photoelectrochemical sensor for naproxen determination in sewage, Electroanalysis 32 (9) (2020) 1930–1937.

[100] M. Kanagasabapathy, R. Sekar, Chronopotentiometric/chronoamperometric transient analysis of naproxen via electrochemically synthesized nano spinel ZnFe2O4 films, J. Electroanal. Chem. 832 (2019) 59–68.

[101] A. Afkhami, F. Kafrashi, M. Ahmadi, T. Madrakian, A new chiral electrochemical sensor for the enantioselective recognition of naproxen enantiomers using l-cysteine self-assembled over gold nanoparticles on a gold electrode, RSC Adv. 5 (72) (2015) 58609–58615.

[102] B. Mutharani, P. Ranganathan, S.-M. Chen, C. Karuppiah, Simultaneous voltammetric determination of acetaminophen, naproxen, and theophylline using an in-situ polymerized poly (acrylic acid) nanogel covalently grafted onto a carbon black/La 2 O 3 composite, Microchim. Acta 186 (2019) 1–11.

[103] M. Ghanavati, F. Tadayon, A. Basiryanmahabadi, N.T. Fard, E. Smiley, Design of new sensing layer based on ZnO/NiO/Fe3O4/MWCNTs nanocomposite for simultaneous electrochemical determination of Naproxen and Sumatriptan, J. Pharmaceut. Biomed. Anal. 223 (2023) 115091.

[104] B. Healy, T. Yu, D.C. da Silva Alves, C. Okeke, C.B. Breslin, Cyclodextrins as supramolecular recognition systems: applications in the fabrication of electrochemical sensors, Materials 14 (7) (2021) 1668.

[105] S.V. Kurkov, T. Loftsson, Cyclodextrins, International journal of pharmaceutics 453 (1) (2013) 167–180.

[106] K.-H. Frömming, J. Szejtli, Cyclodextrins in Pharmacy, Springer Science & Business Media, 1993.

[107] S. Tarahomi, G.H. Rounaghi, L. Daneshvar, A novel disposable sensor based on gold digital versatile disc chip modified with graphene oxide decorated with Ag nanoparticles/β-cyclodextrin for voltammetric measurement of naproxen, Sensor. Actuator. B Chem. 286 (2019) 445–450.

[108] M. Shamsipur, H.R. Rajabi, S.M. Pourmortazavi, M. Roushani, Ion imprinted polymeric nanoparticles for selective separation and sensitive determination of zinc ions in different matrices, Spectrochim. Acta Mol. Biomol. Spectrosc. 117 (2014) 24–33.

[109] M. Goudarzi, M. Salavati-Niasari, M. Bazarganipour, M. Motaghedifard, Sonochemical synthesis of Tl 2 O 3 nanostructures: supported on multi-walled carbon nanotube modified electrode for monitoring of copper ions, J. Mater. Sci. Mater. Electron. 27 (2016) 3675–3682.

[110] T. Hishiya, H. Asanuma, M. Komiyama, Molecularly imprinted cyclodextrin polymers as stationary phases of high performance liquid chromatography, Polymer journal 35 (5) (2003) 440–445.

[111] A.O. Santini, J.E.d. Oliveira, H.R. Pezza, L. Pezza, A novel potentiometric naproxenate ion sensor immobilized in a graphite matrix for determination of naproxen in pharmaceuticals, J. Braz. Chem. Soc. 17 (2006) 785–791.

[112] J. Lenik, Preparation and study of a naproxen ion-selective electrode, Mater. Sci. Eng. C 33 (1) (2013) 311–316.

[113] A. Herrera-Chacón, X. Cetó, M. Del Valle, Molecularly imprinted polymers-towards electrochemical sensors and electronic tongues, Anal. Bioanal. Chem. 413 (2021) 6117–6140.

[114] M. Jafari, J. Tashkhourian, G. Absalan, Electrochemical sensor for enantioselective recognition of naproxen using LCysteine/reduced graphene oxide modified glassy carbon electrode, Analytical and Bioanalytical Chemistry Research 7 (2020) 1–15.

[115] N. Adhoum, L. Monser, M. Toumi, K. Boujlel, Determination of naproxen in pharmaceuticals by differential pulse voltammetry at a platinum electrode, Anal. Chim. Acta 495 (1–2) (2003) 69–75.

[116] J. Tashkhourian, B. Hemmateenejad, H. Beigizadeh, M. Hosseini-Sarvari, Z. Razmi, ZnO nanoparticles and multiwalled carbon nanotubes modified carbon paste electrode for determination of naproxen using electrochemical techniques, J. Electroanal. Chem. 714 (2014) 103–108.

[117] C.-M. Hung, C.-P. Huang, C.-W. Chen, C.-D. Dong, A poly-(L-serine)/reduced graphene oxide–Nafion supported on glassy carbon (PLS/rGO− Nafion/GCE) electrode for the detection of naproxen in aqueous solutions, Environ. Sci. Pollut. Control Ser. 29 (9) (2022) 12450–12461.

[118] V. Suryanarayanan, Y. Zhang, S. Yoshihara, T. Shirakashi, Voltammetric assay of naproxen in pharmaceutical formulations using boron-doped diamond electrode, Electroanalysis, An International Journal Devoted to Fundamental and Practical Aspects of Electroanalysis 17 (11) (2005) 925–932.

[119] G. Aguilar-Lira, A. Rojas-Hernández, J. Rodriguez, M. Páez-Hernández, G. Álvarez-Romero, Optimized quantification of naproxen based on DPV and a multiwalled MWCNT-carbon paste electrode, J. Electrochem. Soc. 167 (16) (2020) 166510.

[120] A. Lapresta-Fernandez, P.J. Cywinski, A.J. Moro, G.J. Mohr, Fluorescent polyacrylamide nanoparticles for naproxen recognition, Anal. Bioanal. Chem. 395 (2009) 1821–1830.

[121] G. Li, R. Jin, Gold nanocluster-catalyzed semihydrogenation: a unique activation pathway for terminal alkynes, J. Am. Chem. Soc. 136 (32) (2014) 11347–11354.

[122] Y. Tao, M. Li, J. Ren, X. Qu, Metal nanoclusters: novel probes for diagnostic and therapeutic applications, Chem. Soc. Rev. 44 (23) (2015) 8636–8663.

[123] M. Jafari, J. Tashkhourian, G. Absalan, Chiral recognition of naproxen enantiomers based on fluorescence quenching of bovine serum albumin–stabilized gold nanoclusters, Spectrochim. Acta Mol. Biomol. Spectrosc. 185 (2017) 77–84.

[124] E. Tereshatov, M.Y. Boltoeva, C. Folden, First evidence of metal transfer into hydrophobic deep eutectic and low-transition-temperature mixtures: indium extraction from hydrochloric and oxalic acids, Green Chem. 18 (17) (2016) 4616–4622.

[125] Q. Yin, M. Wang, D. Fang, Y. Zhu, L. Yang, N. Novel, Cl-doped deep eutectic solvents-based carbon dots as a selective fluorescent probe for determination of morphine in food, RSC advances 11 (27) (2021) 16805–16813.

[126] R. Tabaraki, F. Nazari, Comparison of carbon dots prepared in deep eutectic solvent and water/deep eutectic solvent: study of fluorescent detection of Fe3+ and cetirizine and their photocatalytic antibacterial activity, Journal of Fluorescence 32 (2) (2022) 549–558.

[127] A.P. Lima, G.L. Nunes, R.G. Franco, R. Mariano-Neto, G.S. Oliveira, E.M. Richter, E. Nossol, R.A. Munoz, Al2O3 microparticles immobilized on glassy-carbon electrode as catalytic sites for the electrochemical oxidation and high detectability of naproxen: experimental and simulation insights, J. Electroanal. Chem. 882 (2021) 114988.

[128] P. Norouzi, F. Dousty, M.R. Ganjali, P. Daneshgar, Dysprosium nanowire modified carbon paste electrode for the simultaneous determination of naproxen and paracetamol: application in pharmaceutical formulation and biological fluid, Int. J. Electrochem. Sci. 4 (10) (2009) 1373–1386.

[129] J.F. Garcia-Reyes, P. Ortega-Barrales, A. Molína-Dlaz, Multicommuted fluorometric multiparameter sensor for simultaneous determination of naproxen and salicylic acid in biological fluids, Anal. Sci. 23 (4) (2007) 423–428.

[130] S. Wang, M. Pan, K. Liu, X. Xie, J. Yang, L. Hong, S. Wang, A SiO2@ MIP electrochemical sensor based on MWCNTs and AuNPs for highly sensitive and selective recognition and detection of dibutyl phthalate, Food Chem. 381 (2022) 132225.

[131] V. Thotathil, N. Sidiq, J.S. Al Marri, S.A. Zaidi, Molecularly imprinted polymer-based sensors integrated with transition metal dichalcogenides (TMDs) and MXenes: a review, Crit. Rev. Anal. Chem. (2023) 1–26.

[132] G. Li, X. Qi, J. Wu, X. Wan, T. Wang, Y. Liu, Y. Chen, Y. Xia, Highly stable electrochemical sensing platform for the selective determination of pefloxacin in food samples based on a molecularly imprinted-polymer-coated gold nanoparticle/black phosphorus nanocomposite, Food Chem. 436 (2024) 137753.

[133] A. Parihar, P. Sharma, N.K. Choudhary, R. Khan, E. Mostafavi, Internet-of-Things-integrated molecularly imprinted polymer-based electrochemical nano-sensors for pesticide detection in the environment and food products, Environmental Pollution (2024) 124029.